# Mechanism of Bactericidal and Fungicidal Activities of Textiles Covalently Modified With Alkylated Polyethylenimine

**Jian Lin,[1] Shuyi Qiu,[1] Kim Lewis,[2] Alexander M. Klibanov[1]**

*[1]Department of Chemistry and Division of Biological Engineering, Massachusetts Institute of Technology, Cambridge, Massachusetts 02139; telephone: 617-253-3556; fax: 617-252-1609; e-mail: klibanov@mit.edu*
*[2]Department of Biology, Northeastern University, Boston, Massachusetts*

*Received 13 November 2002; accepted 16 December 2002*

*DOI: 10.1002/bit.10651*

**Abstract:** Our previous studies have led to a novel "non-release" approach to making materials bactericidal by covalently attaching certain moderately hydrophobic polycations to their surfaces. In the present work, this strategy is extended beyond the heretofore-used nonporous materials to include common woven textiles (cotton, wool, nylon, and polyester). Pieces of such cloths derivatized with *N*-hexylated+methylated high-molecular-weight polyethylenimine (PEI) are strongly bactericidal against several airborne Gram-positive and Gram-negative bacteria. In contrast, the immobilized and *N*-alkylated PEIs of low molecular weight have only a weak, if any, bactericidal activity. These findings support a mechanism of the antibacterial action whereby high-molecular-weight and hydrophobic polycationic chains penetrate bacterial cell membranes/walls and fatally damage them. The bactericidal textiles prepared herein are lethal not only to pathogenic bacteria but to fungi as well. © 2003 Wiley Periodicals, Inc. *Biotechnol Bioeng* **83**: 168–172, 2003.

**Keywords:** polycations; immobilization; microbicidal materials; fibers; cotton; molecular weight of polymers

against a variety of Gram-positive and Gram-negative bacteria, whether airborne or waterborne (Lin et al., 2002a, 2002b; Tiller et al., 2001, 2002). Thus far, however, this approach has been validated for only nonporous materials (Borman, 2002) and only against bacterial pathogens.

The defining mechanistic feature of the aforementioned strategy is that it is *not* based on a gradual release of an entrapped antiseptic agent (Tiller et al., 2001). Similar non-release claims have been made for antibacterial materials developed by other investigators (Borman, 2002; Isquith et al., 1972; www.microbeshield.com), whereby fatty alkyl groups were attached to surfaces via ammonium anchors. However, in contrast to our immobilized *polymers* (Lin et al., 2002a, 2002b; Tiller et al., 2001, 2002), it is difficult to imagine how these relatively short chains can fatally penetrate bacterial membranes and/or cell walls.

In the present investigation, we extend our bactericidal technology to textiles made of cotton, wool, nylon, or polyester. Moreover, such porous, woven materials bearing co-

## Titration of Primary and Quaternary Amino Groups

*Primary amino groups* (Lee and Loudon, 1979). A 2×2-cm wool cloth was immersed in 2 mL of a 0.1 *M* picric acidsolution in methylene chloride, followed by washing with 20 mL of the solvent, drying, and addition of 2 mL of dry *N*,*N*-diisopropylethylamine The density of the resultant NH2 groups was found to be 0.92 ± 0.02 nmol/cm2

*Quaternary amino groups* (Ledbetter and Bowen, 1969). A 2×2-cm alkyl-PEI-derivatized cloth was dipped in a 1% aqueous solution of fluorescein (Na salt), shaken for 5 min, thoroughly rinsed with distilled water, and placed in 20 mL of a 0.25% aqueous solution of cetyltrimethylammonium chloride. The densities of the quaternary amino groups on the *N*-alkylated PEI-derivatized cotton, wool, nylon, and polyester cloths were found to be 17.3 ± 0.4, 3.9 ± 0.8, 15.9 ± 0.8, and 9.1 ± 0.6 nmol/cm2, respectively.

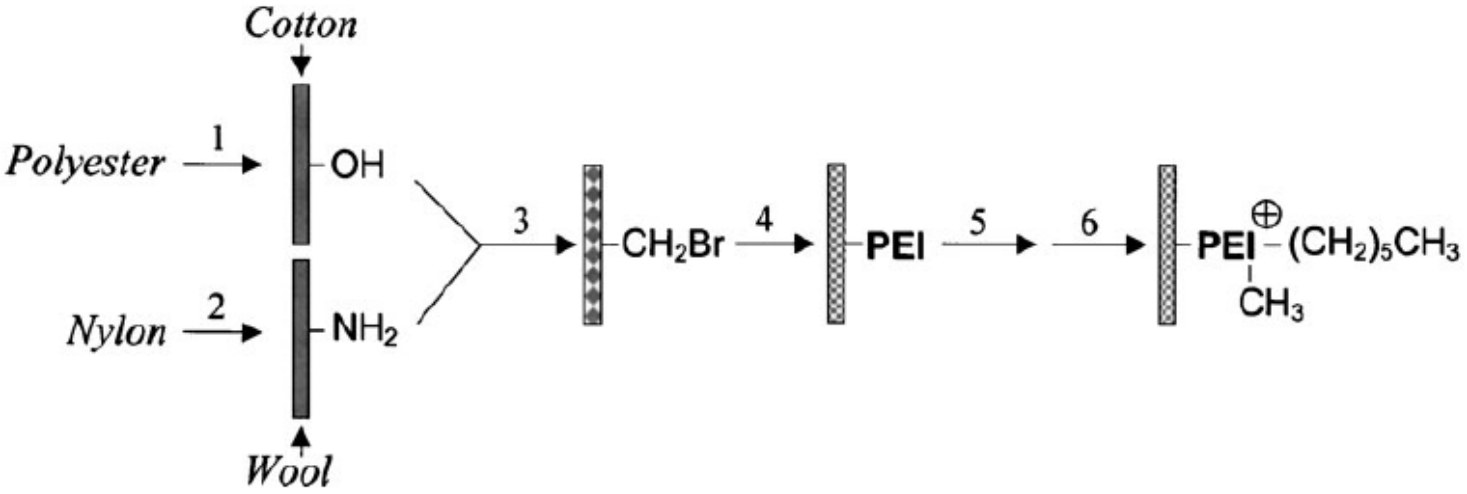


**Figure 1.** Schematic representation of the synthesis of *N*-alkylated PEIs covalently immobilized onto cotton, wool, nylon, or polyester cloths. Step 1: alkaline hydrolysis of polyester [poly(ethylene terephthalate)]; step 2: acid hydrolysis of nylon (Nylon-66); step 3: acylation of original or partially hydrolyzed textiles' hydroxyl or amino groups with 4-bromobutyryl chloride; step 4: covalent attachment (*N*-alkylation) of PEI; step 5: *N*-hexylation of the immobilized PEI with bromohexane; and step 6: *N*-methylation of the immobilized *N*-hexyl-PEI with iodomethane (see text).

**Table I.** Microbicidal efficiencies of four textiles derivatized with *N*-alkylated 750-kDa PEI against airborne bacteria and fungi.[a]

| | | Microbicidal activities (%)[b] | | | |
|---|---|---|---|---|---|
| Microorganism | Type | Cotton | Wool | Nylon | Polyester |
| *S. aureus* | Gram(+) | 98 ± 1 | 94 ± 2 | 96 ± 2 | 93 ± 1 |
| *S. epidermidis* | Gram(+) | 97 ± 1 | 98 ± 1 | 98 ± 1 | 97 ± 1 |
| *E. coli* | Gram(−) | 99 ± 1 | 98 ± 1 | 99 ± 1 | 96 ± 2 |
| *P. aeruginosa* | Gram(−) | 98 ± 1 | 97 ± 1 | 98 ± 1 | 98 ± 1 |
| *S. cerevisiae* | Fungus/yeast | 97 ± 1 | 98 ± 1 | 90 ± 2 | 88 ± 9 |
| *C. albicans* | Fungus/yeast | 96 ± 1 | 96 ± 3 | 91 ± 2 | 92 ± 7 |

[a]Immobilization and *N*-alkylation of PEI were carried out as outlined in Figure 1. For experimental details, see text.

[b]All measurements were done in duplicate with the mean values and standard errors obtained shown.

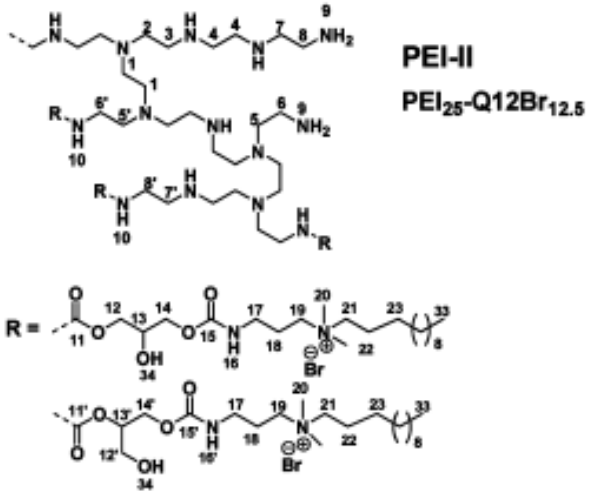

- Next, we explored whether the textiles with immobilized 750-kDa *N*-alkyl-PEI would be effective against airborne fungi. (Fungi/yeasts have a single membrane covered by a thick cell wall composed of glucan and chitin. This design is similar to the cell envelope of Gram-positive bacteria,composed of a membrane covered with a peptidoglycan wall. In Gram-negative bacteria, an additional outer membrane is found above the peptidoglycan wall [Lewis, 2001].)

**Table I.** Microbicidal efficiencies of four textiles derivatized with *N*-alkylated 750-kDa PEI against airborne bacteria and fungi.[a]

| Microorganism | Type | Microbicidal activities (%)[b] | | | |
|---|---|---|---|---|---|
| | | Cotton | Wool | Nylon | Polyester |
| *S. aureus* | Gram(+) | 98 ± 1 | 94 ± 2 | 96 ± 2 | 93 ± 1 |
| *S. epidermidis* | Gram(+) | 97 ± 1 | 98 ± 1 | 98 ± 1 | 97 ± 1 |
| *E. coli* | Gram(−) | 99 ± 1 | 98 ± 1 | 99 ± 1 | 96 ± 2 |
| *P. aeruginosa* | Gram(−) | 98 ± 1 | 97 ± 1 | 98 ± 1 | 98 ± 1 |
| *S. cerevisiae* | Fungus/yeast | 97 ± 1 | 98 ± 1 | 90 ± 2 | 88 ± 9 |
| *C. albicans* | Fungus/yeast | 96 ± 1 | 96 ± 3 | 91 ± 2 | 92 ± 7 |

[a]Immobilization and *N*-alkylation of PEI were carried out as outlined in Figure 1. For experimental details, see text.

[b]All measurements were done in duplicate with the mean values and standard errors obtained shown.

**Table II.** Bactericidal potencies against airborne *S. aureus* of cotton-immobilized and *N*-alkylated PEIs of different molecular weights as a function of washing.[a]

| Molecular weight of PEI (kDa) | Bactericidal activities (%) after: | | |
|---|---|---|---|
| | Regular wash[b] | First exhaustive wash[c] | Second exhaustive wash[c] |
| 750 | 98 ± 1 | 98 ± 1 | 95 ± 3 |
| 25 | 83 ± 3 | 75 ± 11 | 70 ± 6 |
| 2 | 53 ± 17 | 35 ± 15 | 37 ± 8 |
| 0.8 | 58 ± 10 | 24 ± 4 | 19 ± 13 |

[a]See footnotes to Table I.

[b]Consisted of washing with methanol and distilled water.

[c]Consisted of additional stirring in soapy water at 55°C overnight, followed by thorough rinsing with distilled water.

One can see that neither the first nor the second cycle had any appreciable effect on the bactericidal potency of the cottonimmobilized and *N*-alkylated 750-kDa PEI (first row in Table II). (Likewise, this exhaustive washing of the *N*alkylated high-molecular-weight PEI immobilized onto wool, nylon, and polyester did not noticeably diminish the bactericidal potency.) In contrast, this washing substantially cut the bactericidal efficiencies of the immobilized and *N*alkylated PEIs of smaller sizes.

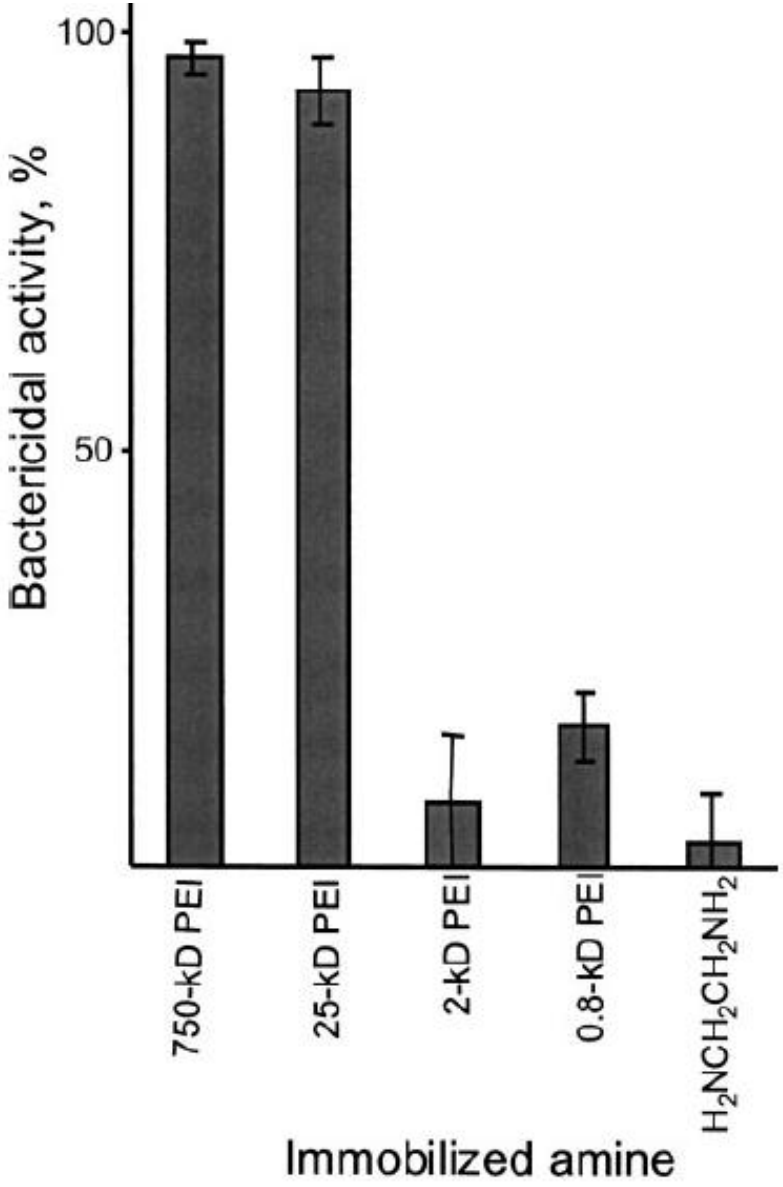


**Figure 2.** Bactericidal activities against airborne *S. aureus* of the *N*-alkylated PEIs of different molecular weights, as well as of 1,2-diaminoethane, covalently attached (as in Fig. 1) to $NH_2$-glass slides (see text).

It should be emphasized that fatty alkyl chains attached to surfaces through quaternary amine anchors in the reported alternative antibacterial materials (Borman, 2002; Isquith et al., 1972; www.microbeshield.com) are far shorter than even the 0.8-kDa PEI. Therefore, such materials *cannot* function via the same “hole-poking” mechanism as described in this study and elsewhere (Lin et al., 2002a, 2002b; Morgan et al., 2000; Tiller et al., 2001, 2002).

Biomacromolecules

ARTICLE

pubs.acs.org/Biomac

# Recyclable Antibacterial Magnetic Nanoparticles Grafted with Quaternized Poly(2-(dimethylamino)ethyl methacrylate) Brushes

Hongchen Dong,[†] Jinyu Huang,[‡] Richard R. Koepsel,[§] Penglin Ye,[†] Alan J. Russell,[*,§] and Krzysztof Matyjaszewski[*,†]

[†]Carnegie Mellon University, Chemistry Department, Pittsburgh, Pennsylvania 15213, United States

[‡]CIBA Vision Corporation, 11460 Johns Creek Parkway, Duluth, Georgia 30097, United States

[§]Department of Surgery and McGowan Institute for Regenerative Medicine, University of Pittsburgh, Suite 300, 450 Technology Drive, Pittsburgh, Pennsylvania 15219, United States

**ABSTRACT:** Highly efficient recyclable antibacterial magnetite nanoparticles consisting of a magnetic $Fe_3O_4$ core with an antibacterial poly(quaternary ammonium) (PQA) coating were prepared in an efficient four-step process. The synthetic pathway included: (1) preparation of $Fe_3O_4$ nanoparticles via coprecipitation of $Fe^{2+}/Fe^{3+}$ in the presence of an alkaline solution; (2) attachment of an ATRP initiating functionality to the surface of the nanoparticles; (3) surface-initiated atom transfer radical polymerization (ATRP) of 2-(dimethylamino)ethyl methacrylate (DMAEMA); and (4) transformation of PDMAEMA brushes to PQA via quaternization with ethyl bromide. The success of the surface functionalization was confirmed by FT-IR, thermal gravimetric analysis (TGA), elemental analysis, and transmission electron microscopy (TEM). The PQA-modified magnetite nanoparticles were dispersed in water and exhibited a response to an external magnetic field, making the nanoparticles easy to remove from water after antibacterial tests. The PQA-modified magnetite nanoparticles retained 100% biocidal efficiency against *E. coli* ($10^5$ to $10^6$ *E. coli*/mg nanoparticles) during eight exposure/collect/recycle procedures without washing with any solvents or water.

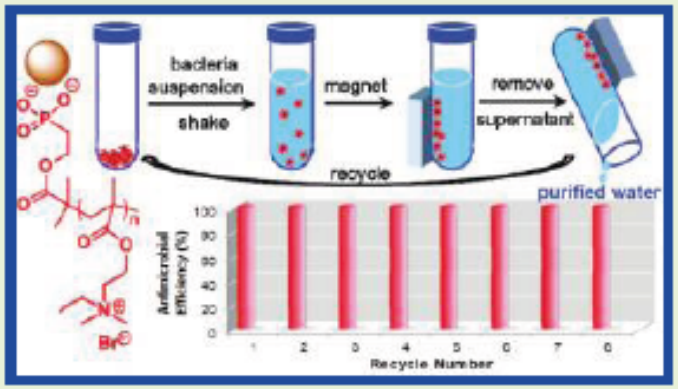

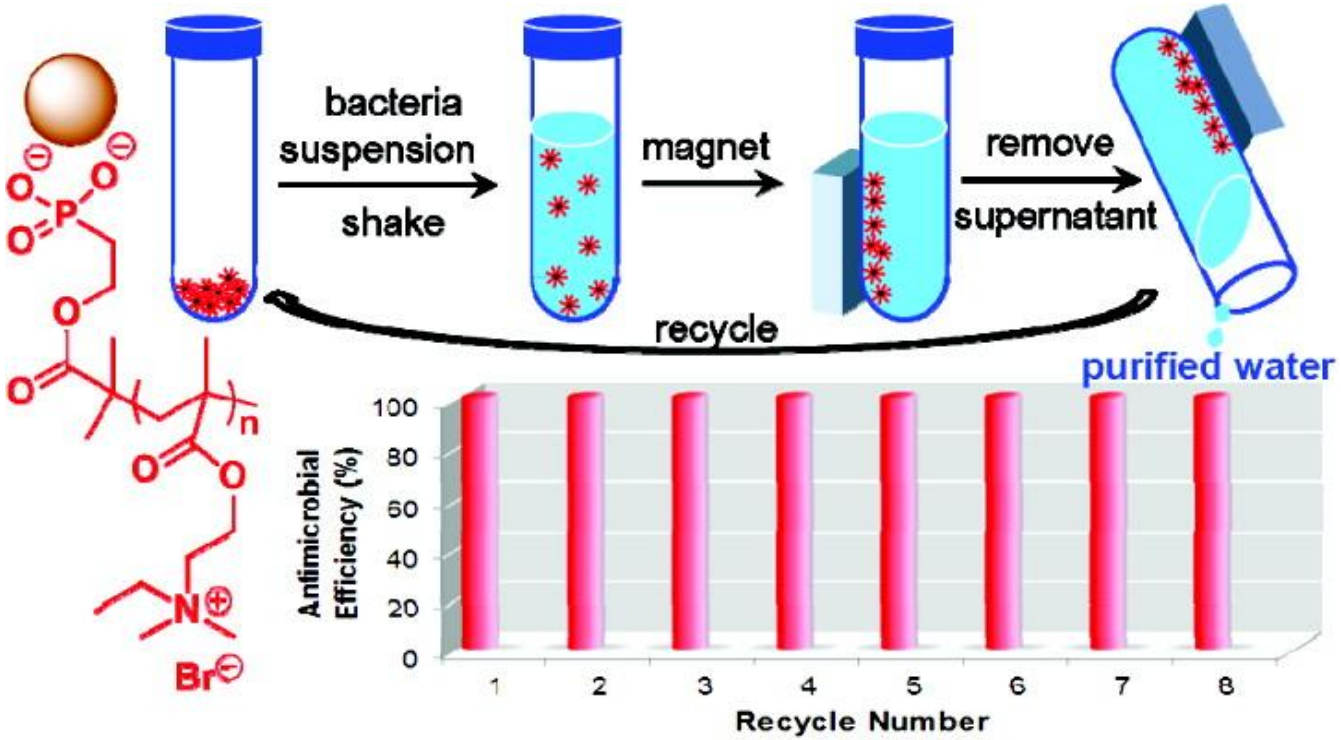

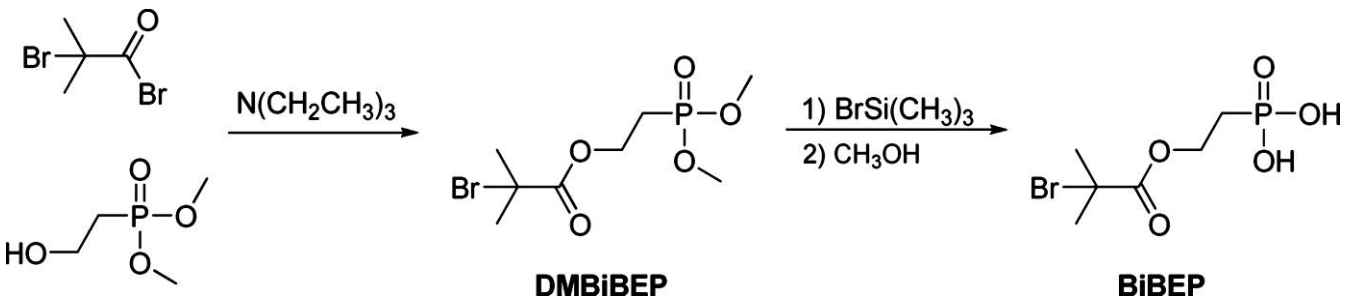






Published in: Hongchen Dong; Jinyu Huang; Richard R. Koepsel; Penglin Ye; Alan J. Russell; Krzysztof Matyjaszewski; *Biomacromolecules* **2011,** 12, 1305-1311.

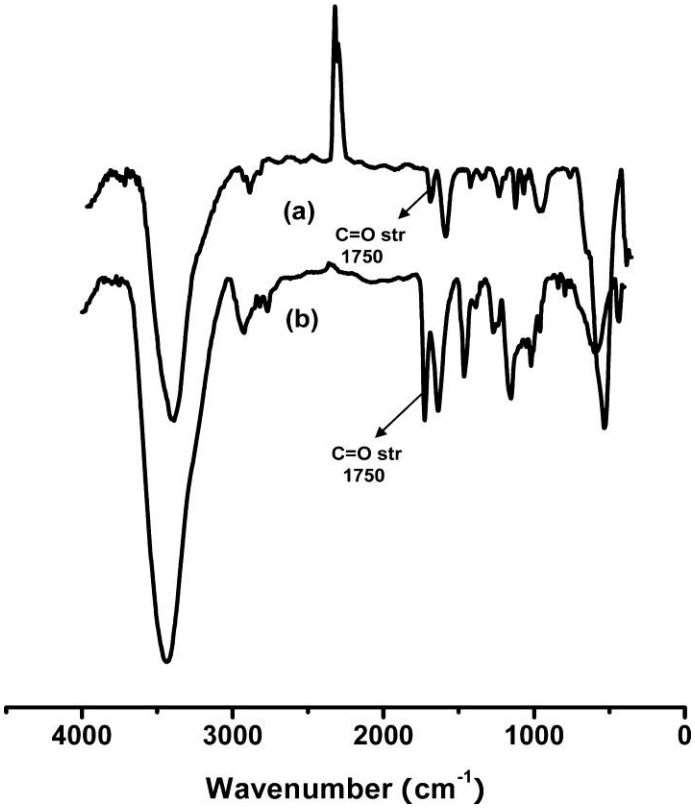


FT-IR spectra of magnetite nanoparticles (a) grafted with ATRP initiator BiBEP and (b) grafted with PDMAEMA.

A characteristic C=O stretch vibration band(1750 cm-1) was clearly observed in the IR spectrum of the modified magnetite nanoparticles.



Published in: Hongchen Dong; Jinyu Huang; Richard R. Koepsel; Penglin Ye; Alan J. Russell; Krzysztof Matyjaszewski; *Biomacromolecules* **2011,** 12, 1305-1311.

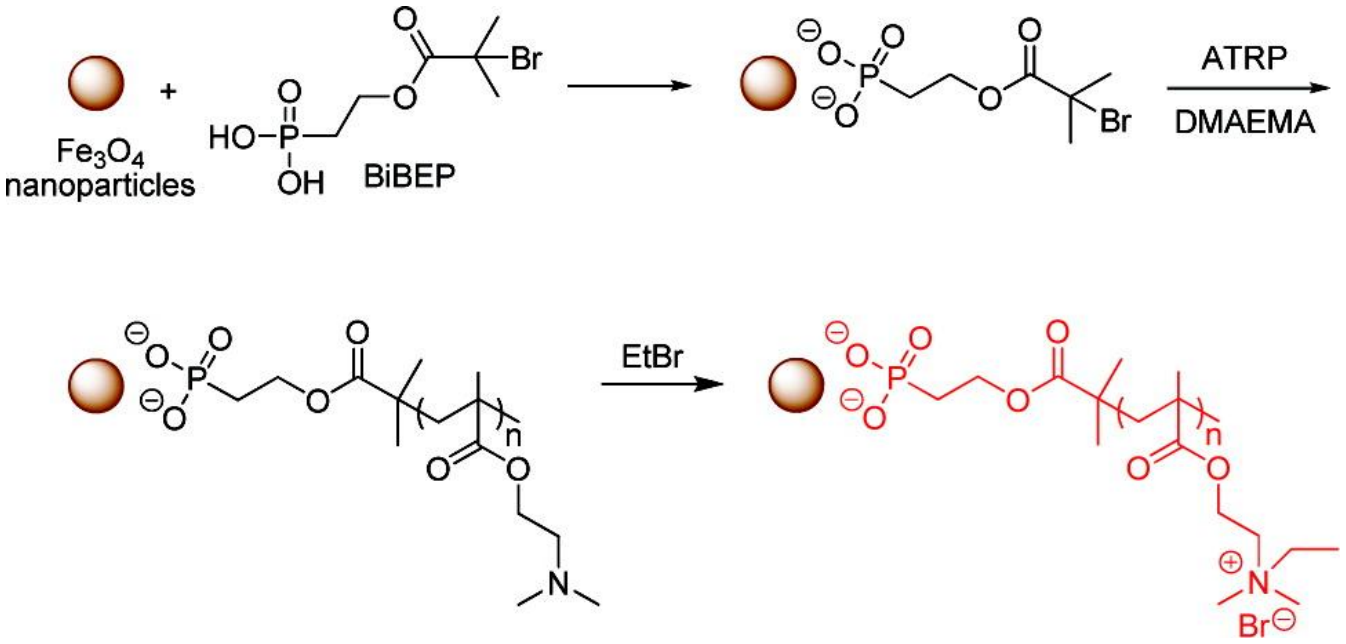

**Table 1. PDMAEMA-Modified Magnetite Nanoparticle**[a]

| entry | $[I]_0/[M]_0/[CuCl]_0/[CuCl_2]_0/[L]_0$[b] | $M_n$ (GPC) | $M_w/M_n$ (GPC) | organic mass (%) (TGA) | organic mass (%) (EA) |
|---|---|---|---|---|---|
| 1 | initiators only | | | 10 | 12 |
| 2 | 1:1570:4.1:0.8:5 | 10 700 | 1.6 | 55 | 50 |
| 3 | 1:1570:4.1:0.8:5 | 44 700 | 1.2 | 61 | 58 |
| 4 | 1:1570:8.2:1.7:10 | 152 100 | 2.1 | 93 | 88 |

[a] GPC: gel permeation chromatography; TGA: thermal gravimetric analysis; EA: elemental analysis. [b] M = DMAEMA; L = HMTETA; $[DMAEMA]_0$ = 5.5 M; solvent: acetone. Polymerization was carried out at 40 °C.

To determine the molecular weight of the tethered chains the magnetite core was etched with hydrochloric acid, and the cleaved polymer chains were characterizedusing GPC.Determination of the Amount of Quaternary Amines on MagnetiteNanoparticles. The density of quaternary ammonium groups onmagnetite nanoparticles was measured as the amount of fluorescein boundper gram of particles. Fluorescein staining of PQA-modified magnetite nanoparticles (Table 1, entry 3) showed that the solvent-accessible densityof quaternary ammonium groups on magnetite nanoparticles was $4.8 \ 10^{19}$/g particles.

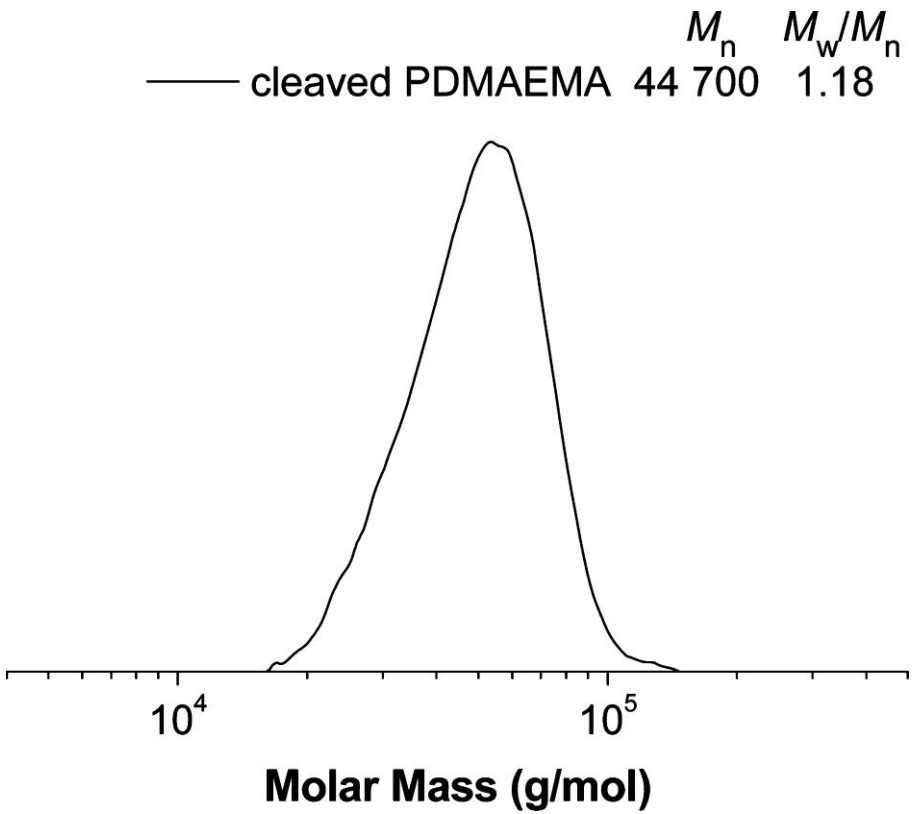


GPC trace of cleaved PDMAEMA chains (Table 1, entry 3).

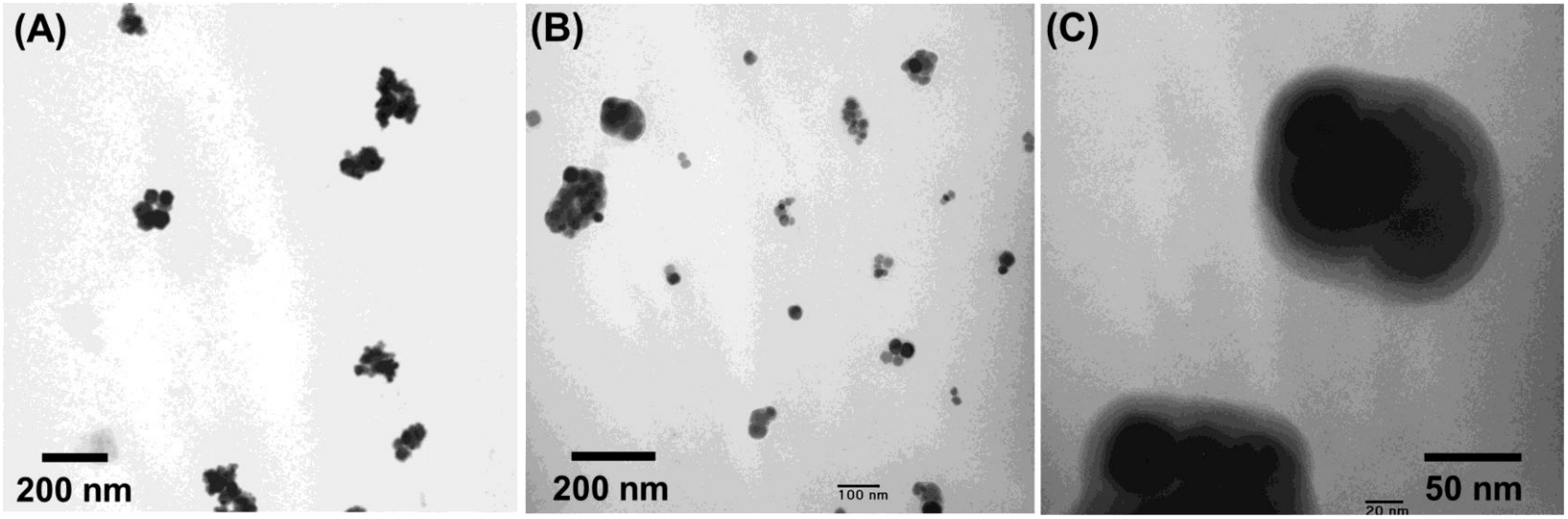


TEM images of (A) the initiator-modified and (B,C) PDMAEMA-grafted magnetite particles (Table 1, entry 3).

The particles described in Table 1, entry 3 were selected for their narrow size range and consistent coating thickness (Figure 3B,C) and for their ready dispersibility in water and toluene and were used for the functional testing.


Published in: Hongchen Dong; Jinyu Huang; Richard R. Koepsel; Penglin Ye; Alan J. Russell; Krzysztof Matyjaszewski; *Biomacromolecules* **2011,** 12, 1305-1311.

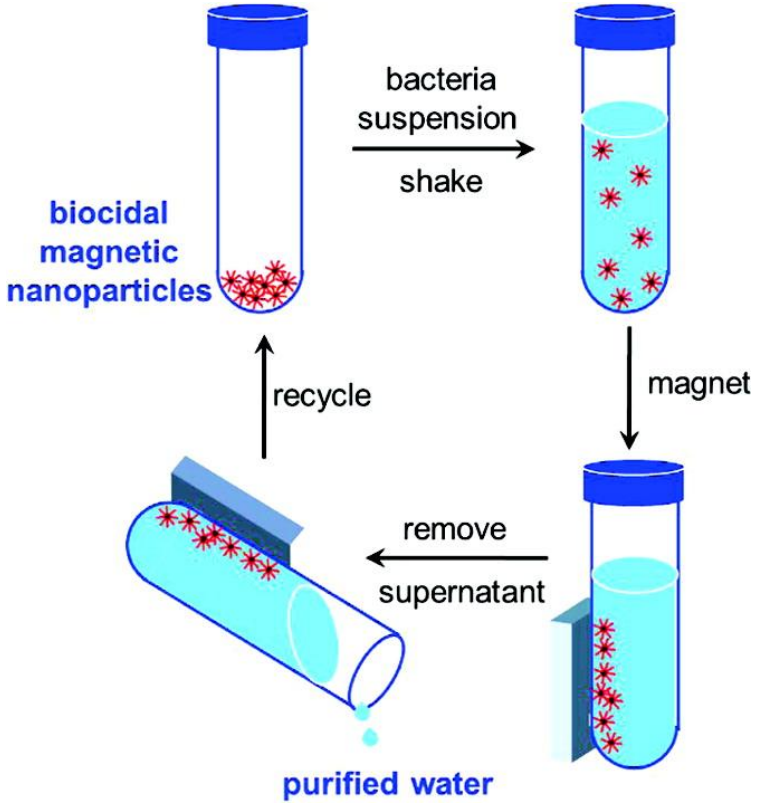


After exposure to an external magnetic field for 20 min, the majority of the nanoparticles were attracted to the source of the magnetic field. However, there was a small portion of magnetite nanoparticles remaining in the supernatant, which could be due to the low mass fraction of magnetite in these hybrid particles.

25.04.2020
Published in: Hongchen Dong; Jinyu Huang; Richard R. Koepsel; Penglin Ye; Alan J. Russell; Krzysztof Matyjaszewski; *Biomacromolecules* **2011,** 12, 1305-1311.

**Table 2. Antimicrobial Activity of PQA-Modified Magnetic Nanoparticles[a]**

| | number of survived *E. coli*/mL | | | antimicrobial efficiency |
|---|---|---|---|---|
| | control[b] | PQA-modified magnetite no. 1[c] | PQA-modified magnetite no. 2[c] | |
| 1st cycle | $2.5 \times 10^5$ | 0 | 0 | 100% |
| 2nd cycle | $2.7 \times 10^5$ | 0 | 0 | 100% |
| 3rd cycle | $3.6 \times 10^5$ | 0 | 0 | 100% |
| 4th cycle | $4.0 \times 10^5$ | 0 | 0 | 100% |
| 5th cycle | $6.9 \times 10^5$ | 0 | 0 | 100% |
| 6th cycle | $6.1 \times 10^5$ | 0 | 0 | 100% |
| 7th cycle | $2.5 \times 10^5$ | 0 | 0 | 100% |
| 8th cycle | $2.8 \times 10^5$ | 0 | 0 | 100% |

[a] Concentration of PQA-modified magnetite particles = 1 mg/mL. [b] Control: bare magnetite particles (1 mg/mL). [c] PQA-modified magnetite nos. 1 and 2 are identical (Table 1, entry 3).

we separated the PQA-modified nanoparticles into two parts based on the response time to an external magnet. One required <10 min and the other needed >10 min.

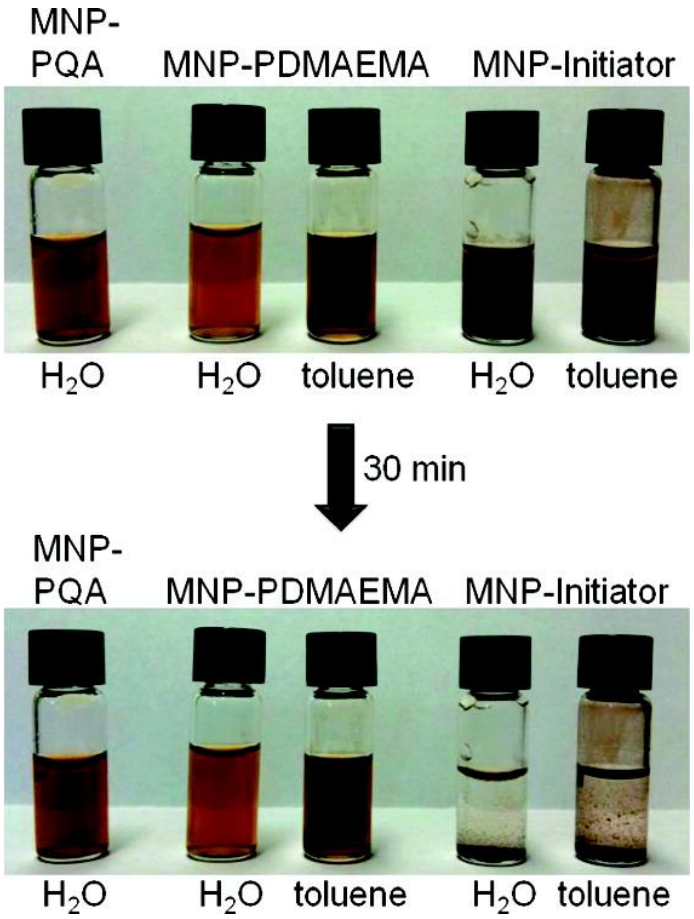


Stability of the suspensions of initiator, PDMAEMA, and PQA-modified nanoparticles in water and toluene (0.5 wt % of nanoparticles, Table 1, entry 3).

The aqueous suspensions of PQA- and PDMAEMA-modified magnetite nanoparticles as well as the toluene suspension of PDMAEMA-modified particles with up to 2 wt % of the nanoparticles remained stable for several months without sedimentation. In contrast, the initiator-modified magnetite nanoparticles precipitated shortly after being dispersed in either solvent.



Published in: Hongchen Dong; Jinyu Huang; Richard R. Koepsel; Penglin Ye; Alan J. Russell; Krzysztof Matyjaszewski; *Biomacromolecules* **2011,** 12, 1305-1311.


Images of PQA-modified nanoparticles (Table 1, entry 3) in water (2 mg/mL) (a) prior to and (b) after exposure to a permanent magnet for 10 min.


Published in: Hongchen Dong; Jinyu Huang; Richard R. Koepsel; Penglin Ye; Alan J. Russell; Krzysztof Matyjaszewski; *Biomacromolecules* **2011,** 12, 1305-1311.

# Permanent, Nonleaching Antibacterial Surfaces. 1. Synthesis by Atom Transfer Radical Polymerization

Sang Beom Lee,[†] Richard R. Koepsel,[‡] Scott W. Morley,[†] Krzysztof Matyjaszewski,[||] Yujie Sun,[§] and Alan J. Russell*[,†,‡,⊥]

*Department of Bioengineering, Department of Chemical and Petroleum Engineering, and Department of Chemistry, University of Pittsburgh, Pittsburgh, Pennsylvania 15260, Department of Surgery, McGowan Institute for Regenerative Medicine, Suite 200, 100 Technology Drive, Pittsburgh, Pennsylvania 15219, and Center for Macromolecular Engineering, Department of Chemistry, 4400 Fifth Avenue, Carnegie Mellon University, Pittsburgh, Pennsylvania 15213*

*Received September 12, 2003; Revised Manuscript Received January 23, 2004*

We have grown an antimicrobial polymer directly on the surfaces of glass and paper using atom transfer radical polymerization (ATRP). The method described here results in potentially permanent nonleaching antibacterial surfaces without the need to chemically graft the antimicrobial material to the substratum. The tertiary amine 2-(dimethylamino)ethyl methacrylate was polymerized directly onto Whatman #1 filter paper or glass slides via atom transfer radical polymerization. Following the polymerization, the tertiary amino groups were quaternized using an alkyl halide to produce a large concentration of quaternary ammonium groups on the polymer-modified surfaces. Incubating the modified materials with either *Escherichia coli* or *Bacillus subtilis* demonstrated that the modified surfaces had substantial antimicrobial capacity. The permanence of the antimicrobial activity was demonstrated through repeated use of a modified glass without significant loss of activity. Quaternary amines are believed to cause cell death by disrupting cell membranes allowing release of the intracellular contents. Atomic force microscopic imaging of cells on modified glass surfaces supports this hypothesis.

**Permanent, Nonleaching Antibacterial Surfaces. 1. Synthesis by Atom Transfer Radical Polymerization; Sang Beom Lee,Richard R. Koepsel,Scott W. Morley,Krzysztof Matyjaszewski, Yujie Sun,and Alan J. Russell,** *Biomacromolecules*, **2004**, *5* (3), pp 877–882
**DOI:** 10.1021/bm034352k
Publication Date (Web): February 27, 2004

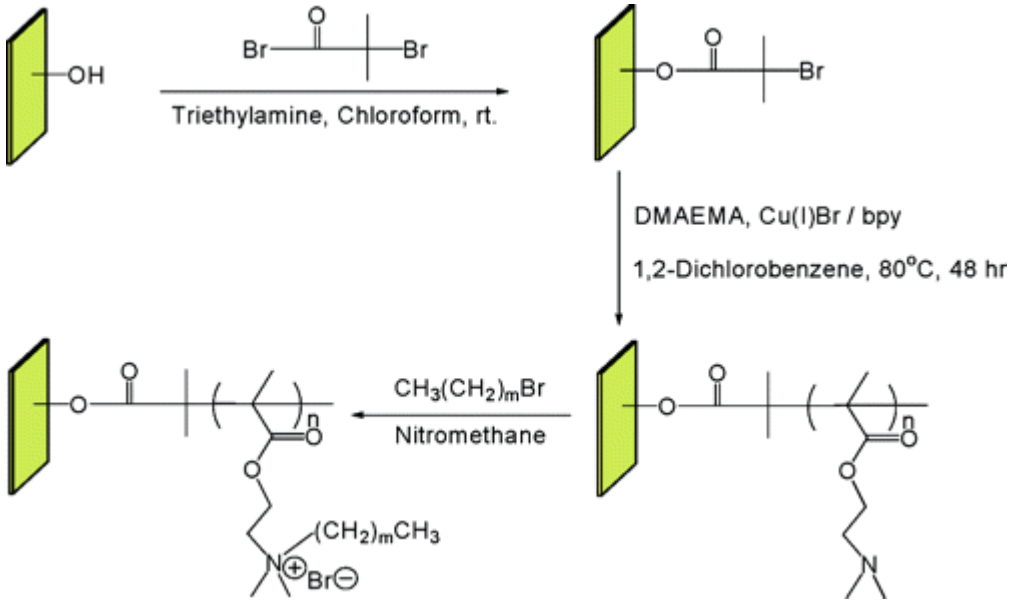

**Scheme 2**

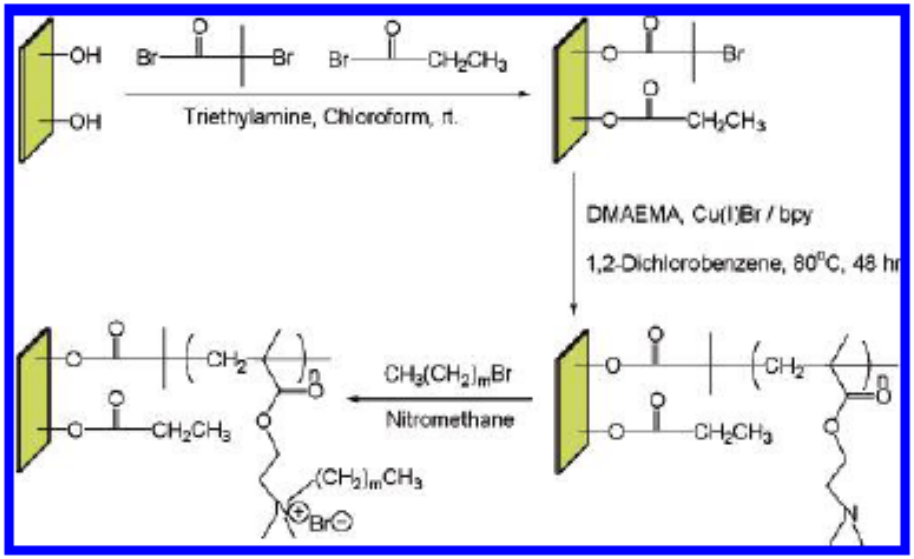


In some experiments, a “blocking agent” was used to synthesize filter papers with varying surfaces densities of the polymer as shown in Scheme 2. The propionyl bromide reacts with the hydroxyl groups found on the filter paper to produce a nonpolymerizable site.

Table 1. Results from GPC after Hydrolysis

| percent of initiator on surface | $M_n$/g mol$^{-1}$ | PDI |
|---|---|---|
| 100 | 21 100 | 2.22 |
| 100[a] | 21 900 | 1.62 |
| 50 | 23 000 | 2.21 |
| 10 | 19 300 | 2.14 |

[a] In the presence of sacrificial initiator.

To determine the molecular weight of the polymers synthesized by this method, papers were prepared with different initiator densities, and the completed polymer chains were cleaved from the surface by HCl hydrolysis. The GPC data for these experiments, presented in Table 1, show that the extent of the polymerization, and thus the length of the polymer chains, and the polydispersity index (PDI) are not greatly influenced by the number of initiation sites.

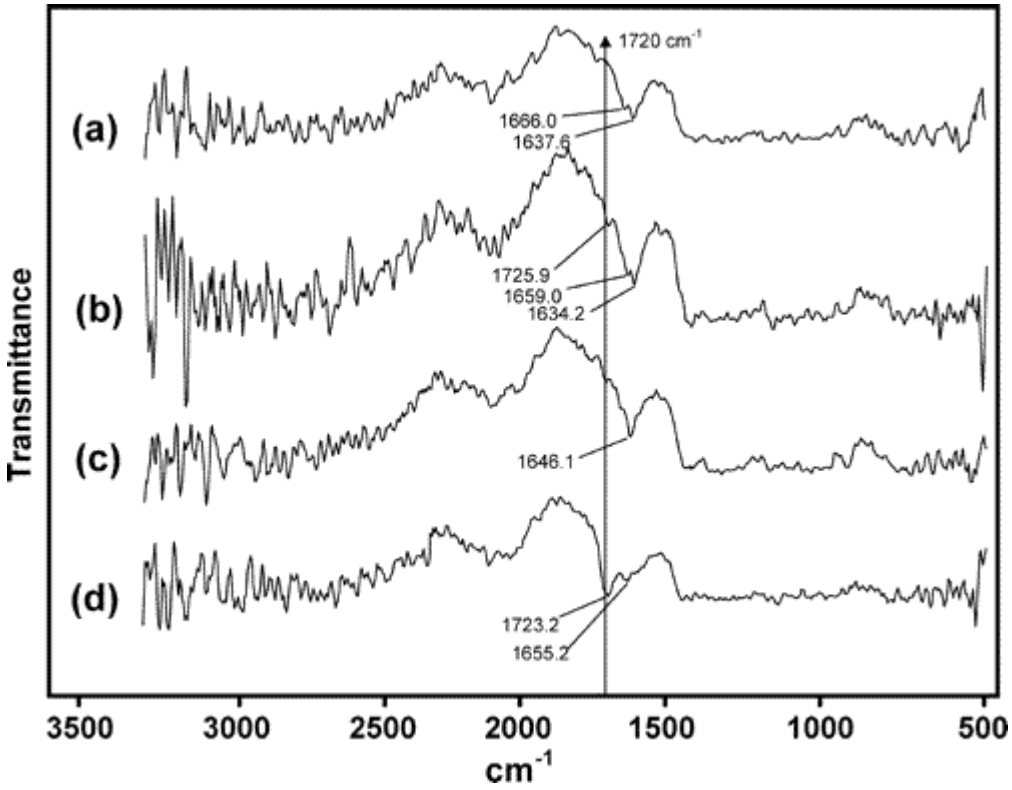


Figure 1 FT-IR of the grafted and ungrafted papers: pure paper (a); pure paper in the presence of sacrificial initiator (b); initiator-modified paper (c); and PDMAEMA-modified paper (d).

A carbonyl peak at 1720 cm-1 is a positive indicator for the poly(2-(dimethylamino)ethyl methacrylate) (PDMAEMA). This carbonyl peak is clearly seen on the grafted paper (Figure 1D) but not on pure paper (Figure 1A) or paper modified with initiator but not subjected to ATRP (Figure 1C).

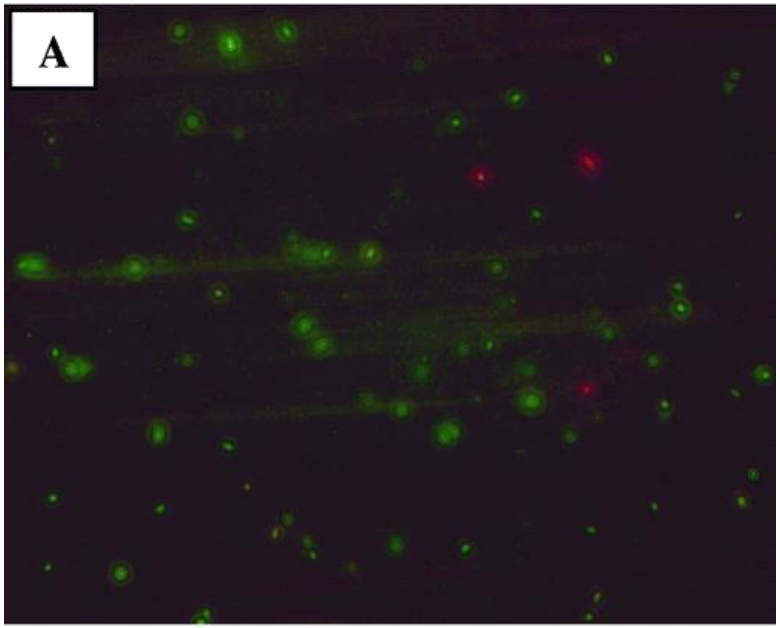


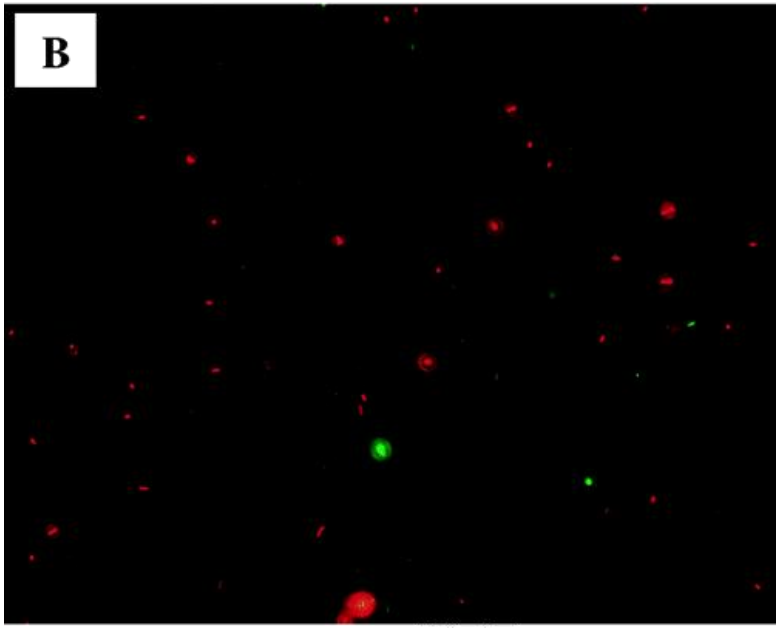


Figure 2 Live/dead analysis of *E. coli* incubated with papers. Panel A. cells incubated with nonmodified paper for 15 min. Panel B. Cells incubated with modified paper for 15 min

The lack of a zone of growth inhibition around any of the paper dots indicated that the material was not diffusing out of the paper. Since the material hydrolyzed from the paper (see Table 1) was no larger that 23 000 Da we believe that we are not washing loose polymer from the paper but are, rather, generating microfibers and small paper pieces with polymer attached to them. Treated glass slides did not release antimicrobialactivity into the buffer when shaken under experimental conditions

Interestingly, when the glass was washed with pure water, the antimicrobial activity disappears after two rounds of exposure to bacteria. Glass washed with SDS retains its antimicrobial activity. Washing the inactivated glass withdetergent resulted in the antimicrobial capacity returning to its original level. It is likely that material from the dead  Cells accumulates on the surface of the glass through a hydrophobic interaction. That  material is then removed by thedetergent with the concomitant restoration of the antimicrobialactivity of the surface. This result agrees with the notion that the mechanism of action of quaternary ammonium involves disruption of the plasma membrane causing the release of intracellular material.

**Table 2.** Antimicrobial Activity of Modified Paper and Glass[a]

| treated sample[b] | organism | number of bacteria added to sample | number of bacteria remaining |
|---|---|---|---|
| paper | *E. coli* | $2.6 \times 10^8$ | 0 |
| paper | *E. coli* | $1.6 \times 10^9$ | $4.9 \times 10^5$ |
| paper | *B. subtilis* | $6.2 \times 10^6$ | $6.0 \times 10^2$ |
| paper | *B. subtilis* spores | $2.5 \times 10^6$ | $1.3 \times 10^6$ |
| glass | *E. coli* | $9.4 \times 10^6$ | $1.4 \times 10^4$ |
| glass | *B. subtilis* | $1.0 \times 10^4$ | 0 |

[a] Samples were incubated with the number of bacteria as indicated. Following incubation the number of viable cells was determined by serial dilution. [b] All samples tested were compared to an untreated control of the same material.

Even though some cells survived, it should be noted that the paper was still extremely effective, killing a total of more than $10^9$ cells within 1 h. It should be noted that because paper is a fibrous material it has a much larger surface area than a piece of glass with the same dimensions. Because of this, a lower number of cells was incubated with the samples (Table 2). Glass samples were tested for their ability to kill *E. coli* and *B. subtilis* vegetative cells. The treated glass killed >9 $10^6$ *E. coli* and > 1 $10^4$ *B. subtilis*.

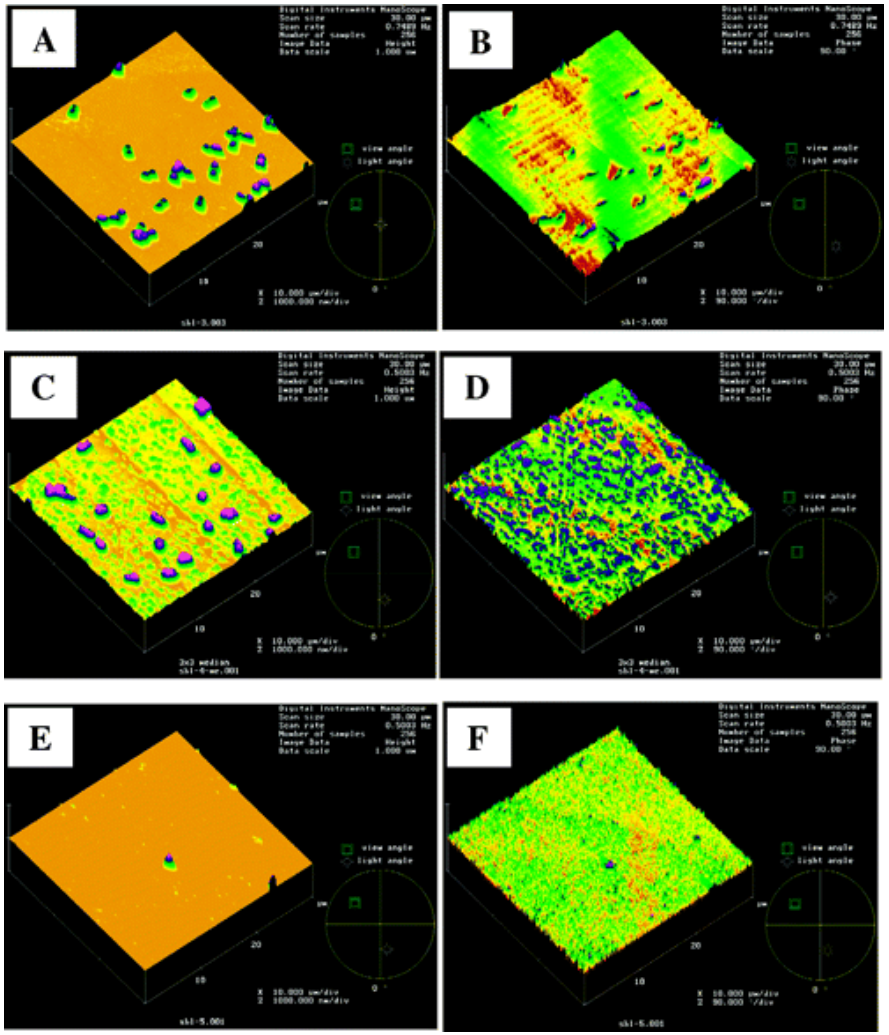


Figure 3 AFM images of glass surfaces. The pictures are: *E. coli* cells on plain glass A and B; *E. coli* cells on quaternized glass C and D; and quaternized glass without added cells E and F. Two data modes are shown for each location, height mode (A, C, and E) and the phase lag mode (B, D, and F). For the height mode, orange is the base color and represents the substrate surface. Relative height progresses through the spectrum with purple indicating the tallest structure. For the phase lag mode, orange represents the largest attraction between the tip and the substrate and purple is the weakest interaction

Quaternary amines are believed to cause cell death by disrupting cell membranes allowing release of the intracellular contents. Atomic force microscopic imaging of cells on modified glass surfaces supports this hypothesis. Perhaps the most interesting result comes from comparison of C and D. Thegreen spots in height mode that indicate the presence of material on the surface have become purple spots in phase lag mode. The fact that the material deposited on the surface has the same lack of attraction to the tip as the intact bacteria suggests that this material is of bacterial origin.

# Antibacterial Polypropylene via Surface-Initiated Atom Transfer Radical Polymerization

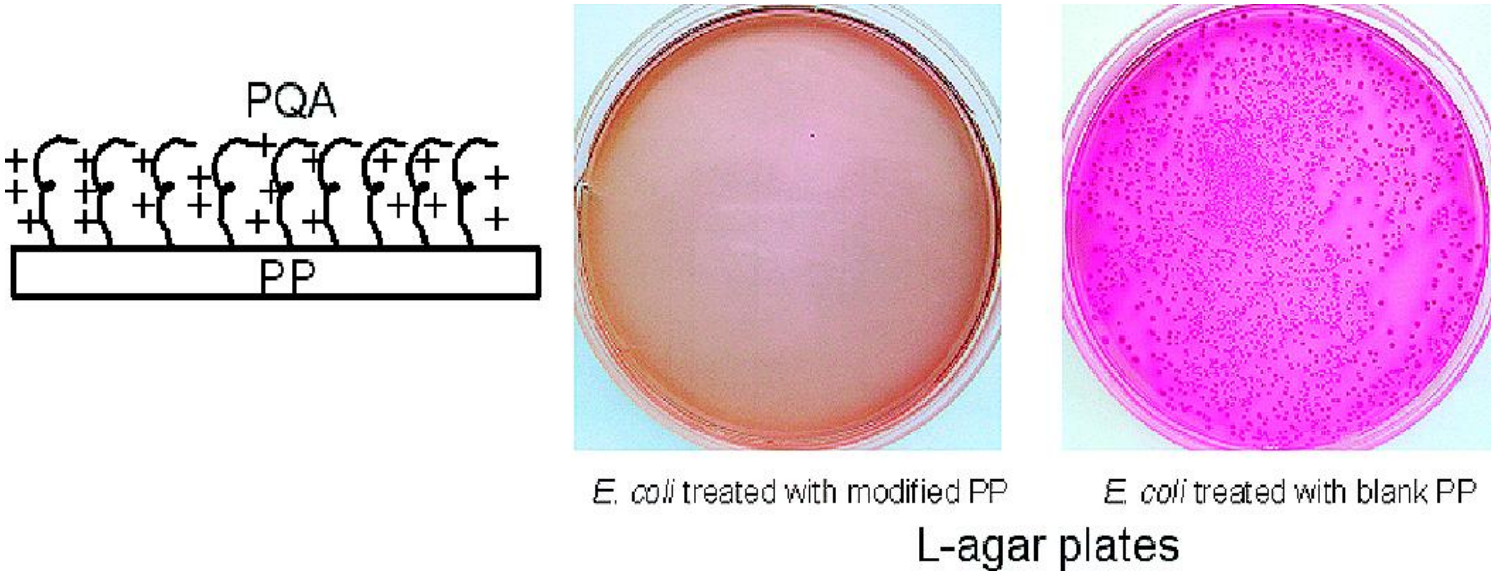


Jinyu Huang,[†] Hironobu Murata,[§] Richard R. Koepsel,[‡] Alan J. Russell,[*] and Krzysztof Matyjaszewski[*†]

Department of Chemistry, Carnegie Mellon University, Pittsburgh, Pennsylvania 15213, and Departments of Chemical and Petroleum Engineering, Bioengineering, and Surgery, McGowan Institute for Regenerative Medicine, Suite 200, 100 Technology Drive, Pittsburgh, Pennsylvania 15219

*Biomacromolecules*, 2007, 8 (5), pp 1396–1399

**DOI:** 10.1021/bm061236j

Publication Date (Web): April 7, 2007

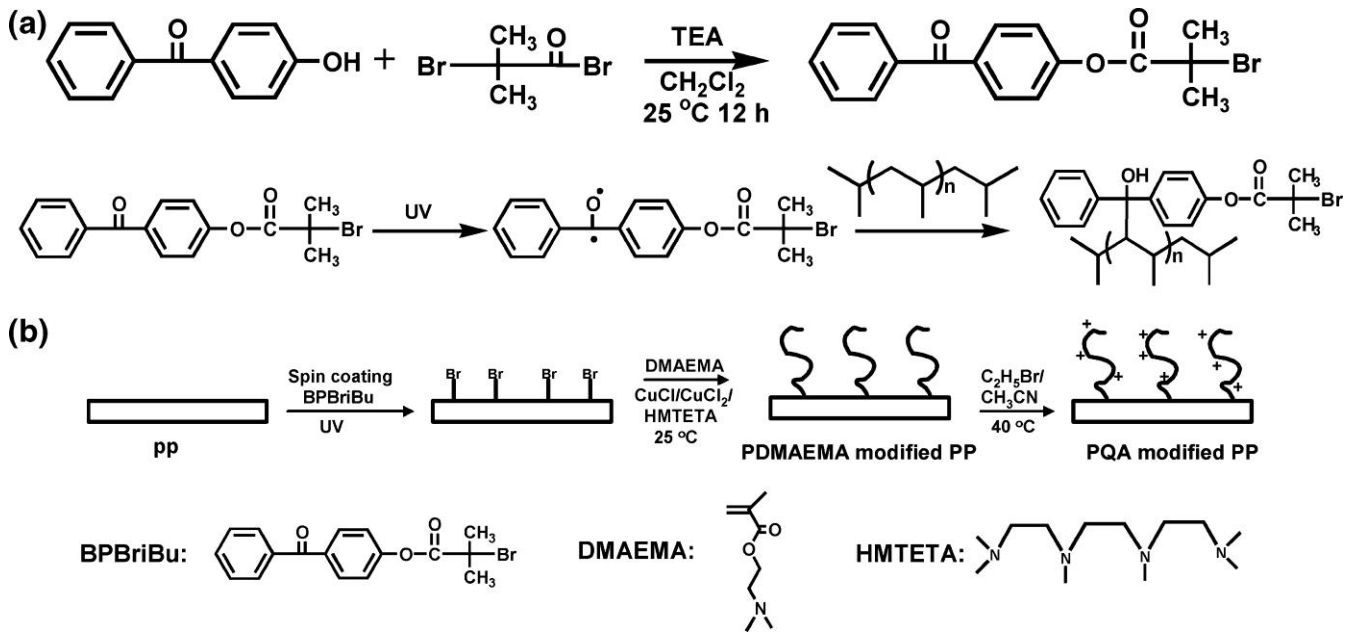


Scheme 1. Synthesis of 2-Benzophenonyl bromoisobutyrate and Benzophenone Chemistry (a) and a Schematic Drawing of Surface-Initiated ATRP of DMAEMA (b)

Published in: Jinyu Huang; Hironobu Murata; Richard R. Koepsel; Alan J. Russell; Krzysztof Matyjaszewski; *Biomacromolecules* **2007,** 8, 1396-1399.
DOI: 10.1021/bm061236j

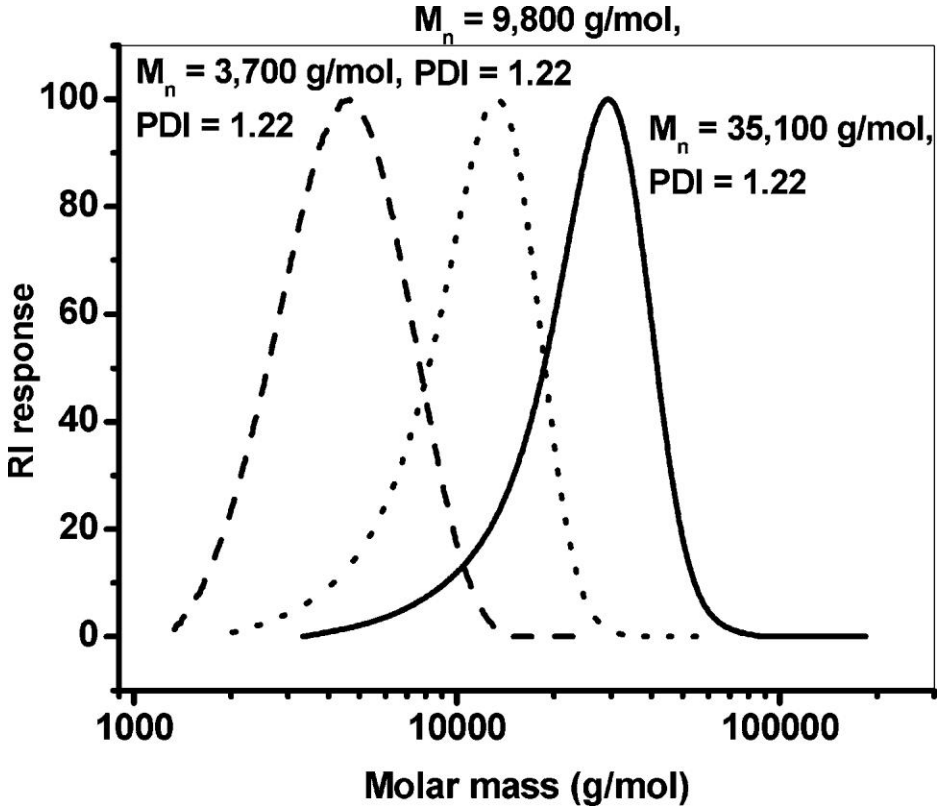


Figure 1 ATRP of DMAEMA initiated from the PP surface. [EBriBu]/[DMAEMA]/[CuCl]/[CuCl2]/[HMTETA] = 1:400:4:0.8:4.8; *V*monomer/*V*acetone = 4:1; *T* = 25 ° C.

Published in: Jinyu Huang; Hironobu Murata; Richard R. Koepsel; Alan J. Russell; Krzysztof Matyjaszewski; *Biomacromolecules* **2007,** 8, 1396-1399.
DOI: 10.1021/bm061236j

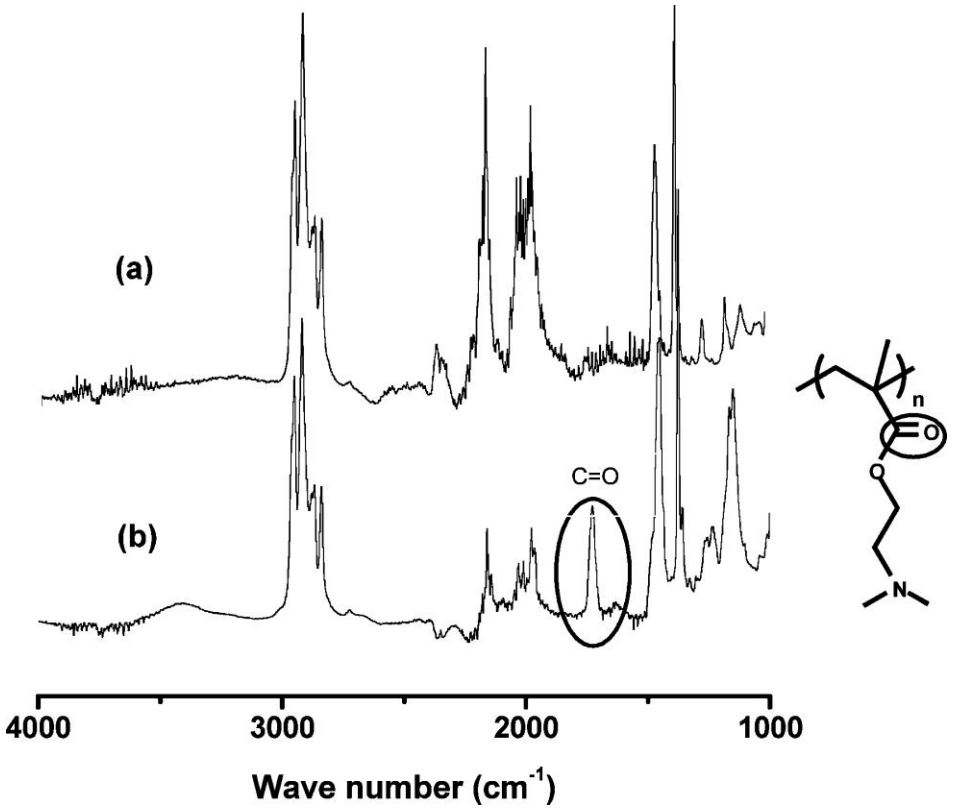


Figure 2 ATR-FTIR spectra of (a) untreated PP and (b) PP modified with PDMAEMA. (*M*n = 35,100 g/mol).

Published in: Jinyu Huang; Hironobu Murata; Richard R. Koepsel; Alan J. Russell; Krzysztof Matyjaszewski; *Biomacromolecules* **2007,** 8, 1396-1399.
DOI: 10.1021/bm061236j

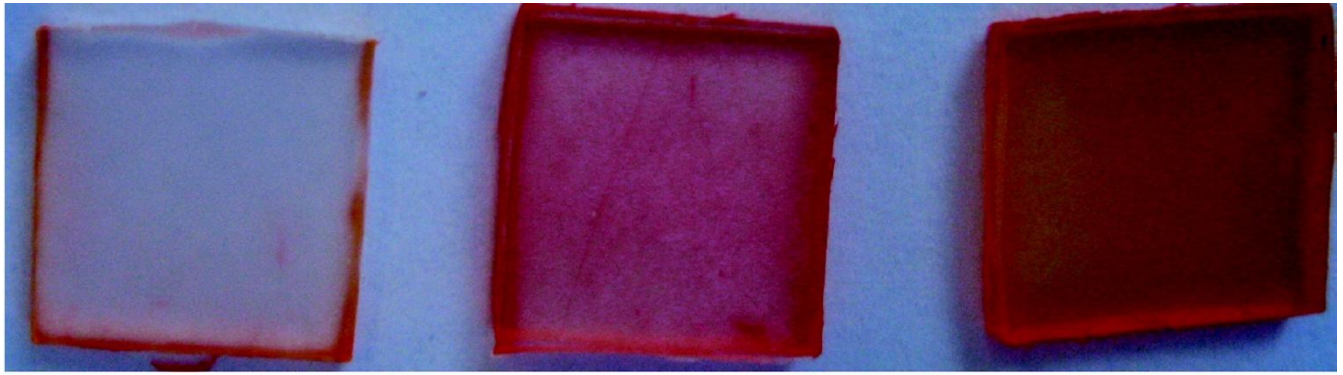


Figure 3 Digital pictures of the PP plates stained with fluorescein salt dye. (a) PP modified with PDMAMEA (*M*n = 1,500 g/mol); (b) PP modified with PDMAMEA (*M*n = 9,800 g/mol); (c) PP modified with PDMAMEA (*M*n = 21,300 g/mol).

Published in: Jinyu Huang; Hironobu Murata; Richard R. Koepsel; Alan J. Russell; Krzysztof Matyjaszewski; *Biomacromolecules* **2007,** 8, 1396-1399.
DOI: 10.1021/bm061236j

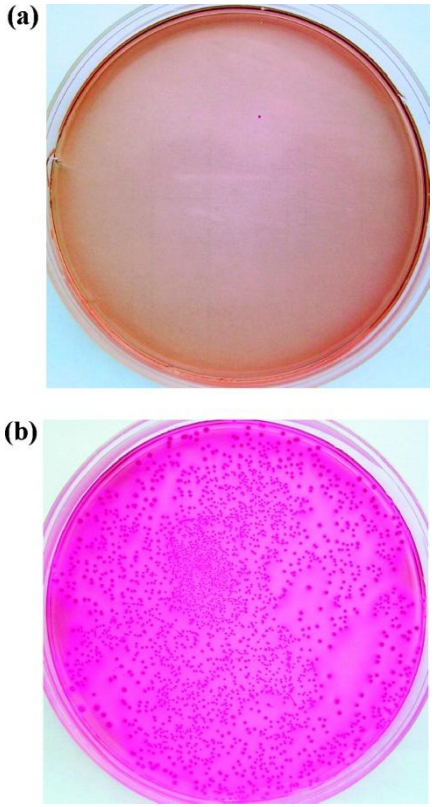


Figure 4 Photographs of l-agar plates onto which the *E. coli* suspension of distilled water treated with the PP slide (entry 3, Table 1) grafted with PQA (a) and the untreated PP slide (b) were deposited and incubated for 24 h. The PP slides were shaken with 5 mL of bacterial suspension for 1 h at 37 ˚ C. The solution was taken, diluted appropriately, and plated on l-agar plates. After overnight incubation, pictures were taken.

Published in: Jinyu Huang; Hironobu Murata; Richard R. Koepsel; Alan J. Russell; Krzysztof Matyjaszewski; *Biomacromolecules* **2007,** 8, 1396-1399.
DOI: 10.1021/bm061236j

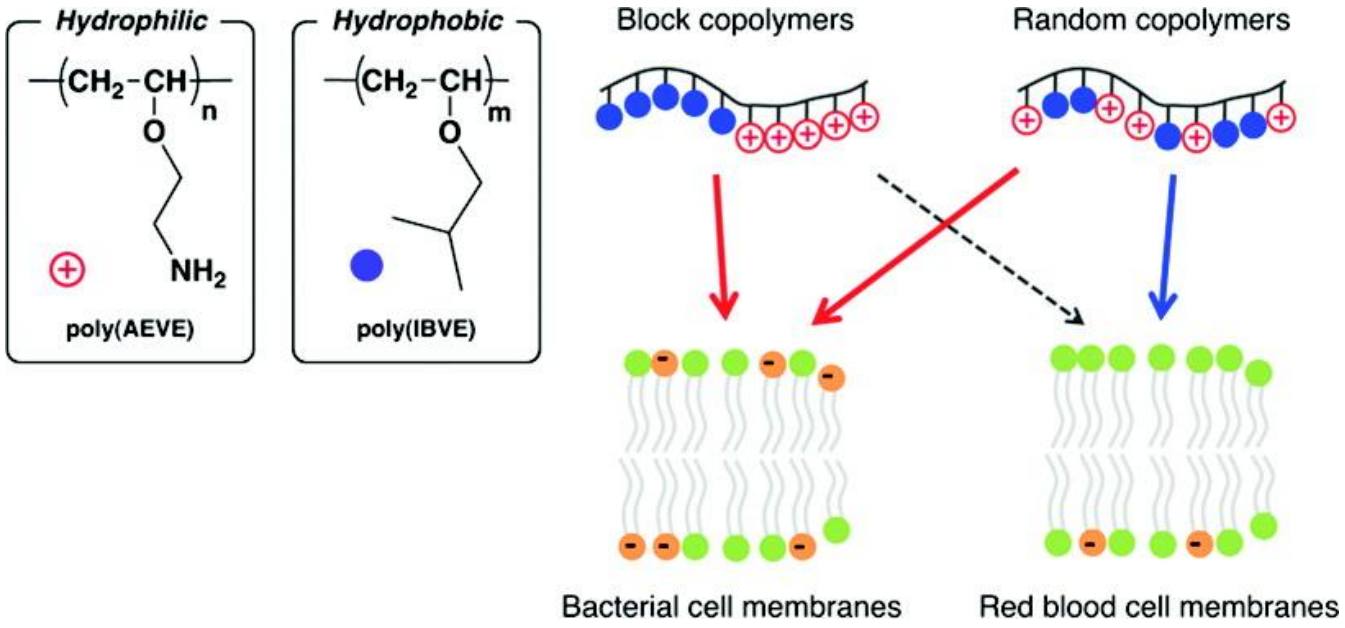


the block copolymers are much less hemolytic compared to the highly hemolytic random copolymers. These results indicate that the amphiphilic copolymer structure is a key determinant of activity

Published in: Yukari Oda; Shokyoku Kanaoka; Takahiro Sato; Sadahito Aoshima; Kenichi Kuroda; *Biomacromolecules* **2011,** 12, 3581-3591.
DOI: 10.1021/bm200780r

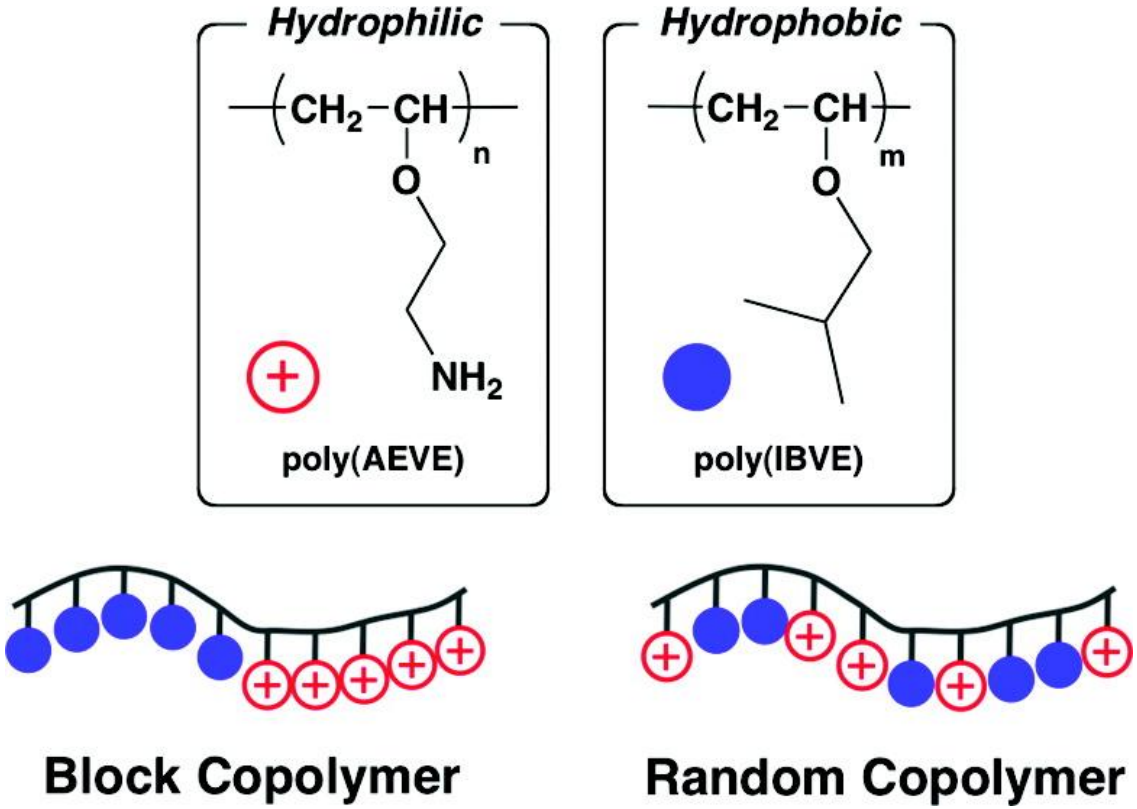


Amphiphilic poly(vinyl ether)s with block and random copolymer structures.

Excess hydrophobicity of polymer chains however, induces their self-association in aqueous media, which would reduce the number of active polymer chains and result in no activity enhancement for polymers with higher compositions of hydrophobic groups

Published in: Yukari Oda; Shokyoku Kanaoka; Takahiro Sato; Sadahito Aoshima; Kenichi Kuroda; *Biomacromolecules* **2011,** 12, 3581-3591.
DOI: 10.1021/bm200780r

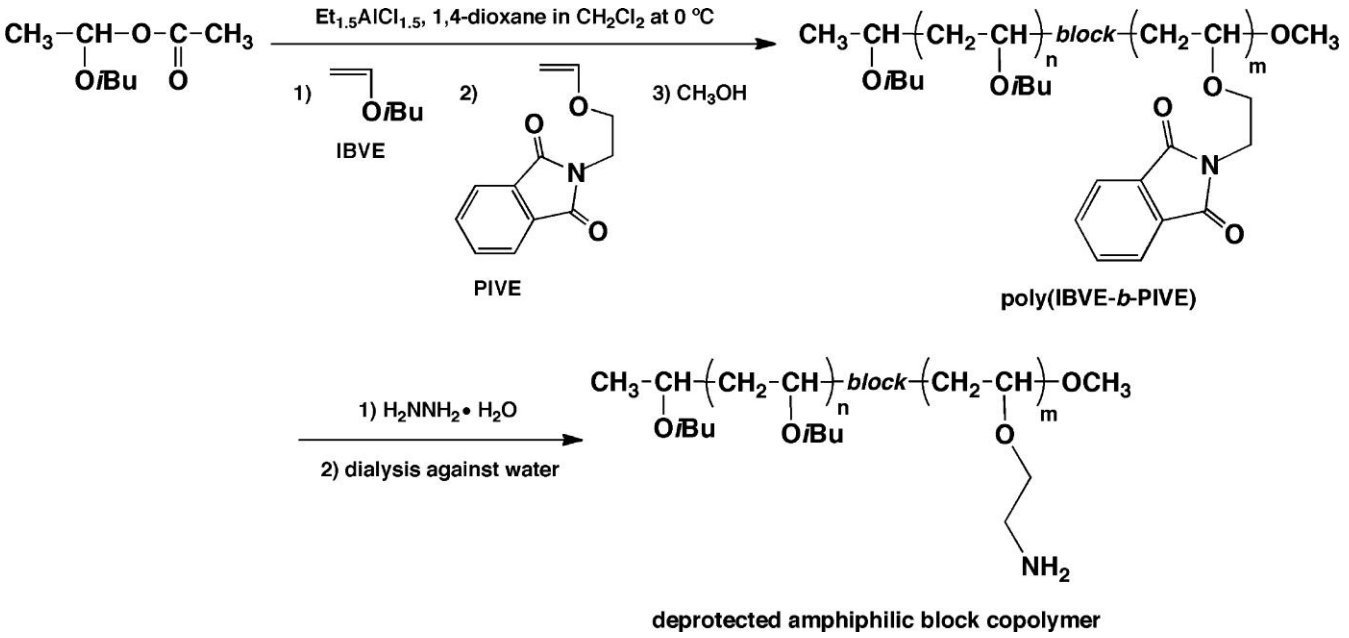


Cationic living polymerization, target is 4000 g/molThe phthalimide protecting groups were removed by treating the polymers with hydrazine, and the crude polymers with primary amine groups were further purified by dialysis against water to remove low MW impurities. $^{1}$H NMR analysis indicated the yield of deprotection was >99%

Published in: Yukari Oda; Shokyoku Kanaoka; Takahiro Sato; Sadahito Aoshima; Kenichi Kuroda; *Biomacromolecules* **2011,** 12, 3581-3591.
DOI: 10.1021/bm200780r

2. $^1$H NMR spectra for precursors of amphiphilic poly(vinyl ether)s and products obtained after deprotection

(A) Homopolymer

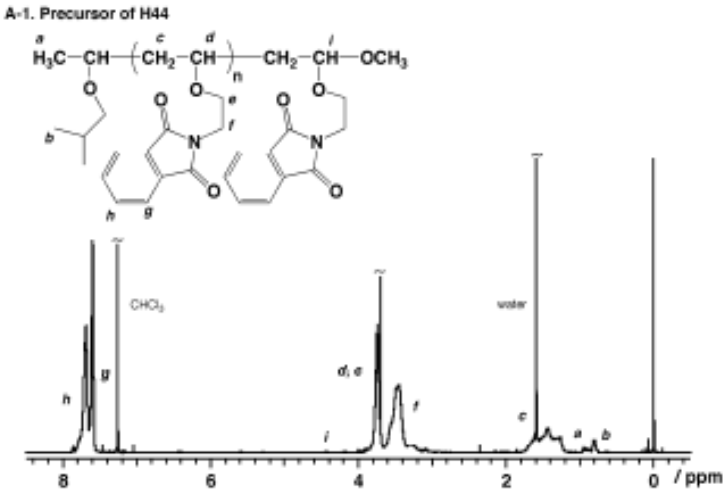


Degree of polymerization (n) was calculated from an integral ratio (*g*, *h*) / (*a*, *b*).

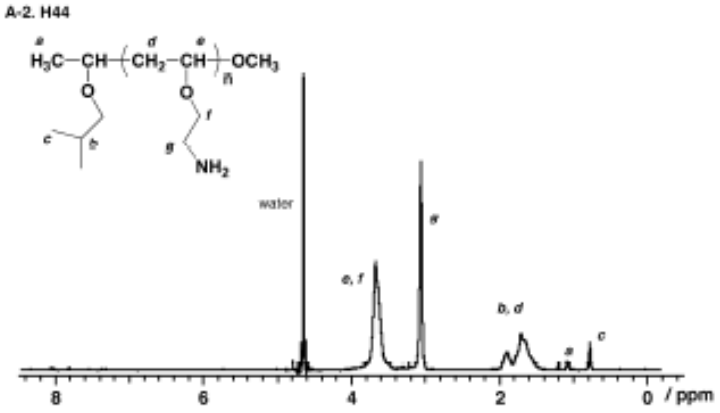


**Figure S2.** $^1$H NMR spectra for the precursor of H44 in $CDCl_3$ (A-1) and H44 in $D_2O$ (A-2).

**1H NMR analysis indicated the yield of deprotection was >99%**

- Preparation of FITC-Labeled Block Copolymer Amphiphilic block copolymer (10 mg, [NH2] = 0.081 mmol) was dissolved in DMF (10 mL) and triethylamine (30 μL, 0.24 mmol). Fluorescein isothiocyanate (FITC, Aldrich) (3.2 mg, 8.1 × 10–3 mmol) in DMF (2 mL) was added into the reaction mixture. The reaction mixture was stirred for 4 h at room temperature in the dark. After the solvent was removed under reduced pressure, the residue was dissolved in methanol. Unreacted FITC was removed by size exclusion chromatography (Sephdex LH-20 gel, Amersham Biosciences, Uppsala, Sweden) using methanol. Comparing the molar absorbance coefficient of F-B3826 and free fluorescein, the average number of FITC molecule per block copolymer chain is 0.45 (Supporting Information). This corresponds to one FITC molecule in 62 amine groups

# protected precursor polymer

| entry | copolymer structure | DP[a] PIVE | DP[a] IBVE | $MP_{IBVE}$[b] (mol %) | $M_n$ (NMR)[c] | $M_w/M_n$ (GPC)[d] | deprotected polymer[e] |
|---|---|---|---|---|---|---|---|
| 1 | homopolymer | 44 (40) | 0 (0) | 0 | 9600 | 1.11 | H44 |
| 2 | random copolymer | 30 (30) | 10 (10) | 25 | 7500 | 1.13 | $R40_{25}$ |
| 3 | | 18 (20) | 20 (20) | 53 | 5900 | 1.14 | $R38_{53}$ |
| 4 | | 8 (10) | 30 (30) | 79 | 4700 | 1.31 | $R38_{79}$ |
| 5 | diblock copolymer | 28 (30) | 10 (10) | 26 | 7100 | 1.16 | $B38_{26}$ |
| 6 | | 19 (20) | 20 (20) | 51 | 6100 | 1.11 | $B39_{51}$ |
| 7 | | 9 (10) | 30 (30) | 77 | 5000 | 1.37 | $B39_{77}$ |
| 8 | | 43 (45) | 15 (15) | 26 | 10800 | 1.19 | $B58_{26}$ |
| 9 | | 58 (60) | 20 (20) | 26 | 14600 | 1.14 | $B78_{26}$ |
| 10 | | 92 (100) | 50 (50) | 35 | 25000 | 1.14 | $B142_{35}$ |

a Calculated by comparing the integral area of signals from the phthalimide group relative to that of the methyl group of the isobutyl group in $^1$H NMR spectra. The theoretical DP based on the feed monomer composition is presented in the parenthe

b Mole percentage of IBVE relative to the total number of monomers in a polymer chain.

c Calculated based on DP and molecular weight of monomeric units.

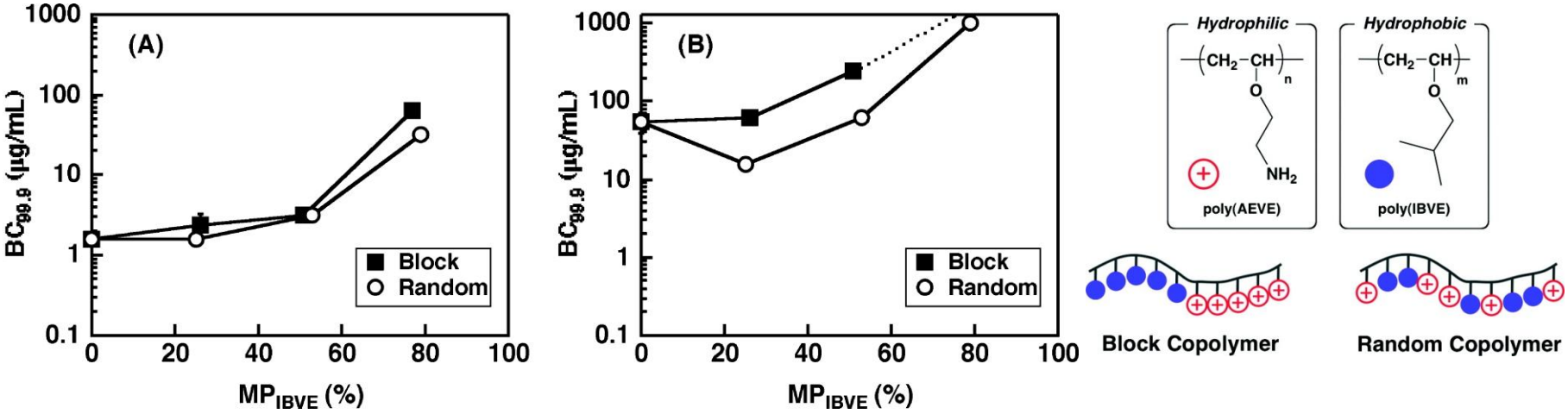


Bactericidal activity (BC99.9) against E. coli of block copolymers (filled squares) and random copolymers (empty circles) with DP ~ 40 as a function of the mole percentage of hydrophobic isobutyl side chains (MPIBVE) in HEPES buffer (A) and MH broth (B). Each data point and error bar represents the average and standard deviation of two independent experiments in duplicate. The BC99.9 value of B3977 in MH broth was over 1000 μg/mL.

The activity reduction by the intramolecular hydrophobic aggregation appears to be more dominant for the random poly(vinyl ether)s than the activity enhancement by hydrophobicity, as found in other polymers. On the other hand, the more rigid polymers (polymethacrylates, polynorbornenes, and polyamides) are likely to have more extended conformations, and the hydrophobic groups would be more exposed to the surrounding aqueous environment. As a result, the more rigid polymers reflect their hydrophobicity more directly on the membrane disruption action, increasing

their antibacterial activity

We further speculated that the decrease in activity of the random poly(vinyl ether)s could be related to the flexible backbone of poly(vinyl ether)s, which would allow the hydrophobic side chains to associate in aqueous solution more easily compared to more rigid polymers. Therefore, the flexible poly(vinyl ether) chains could facilitate the formation of intramolecular aggregates, which reduce the number of active polymer chains against bacteria.

Published in: Yukari Oda; Shokyoku Kanaoka; Takahiro Sato; Sadahito Aoshima; Kenichi Kuroda; *Biomacromolecules* **2011,** 12, 3581-3591.
DOI: 10.1021/bm200780r

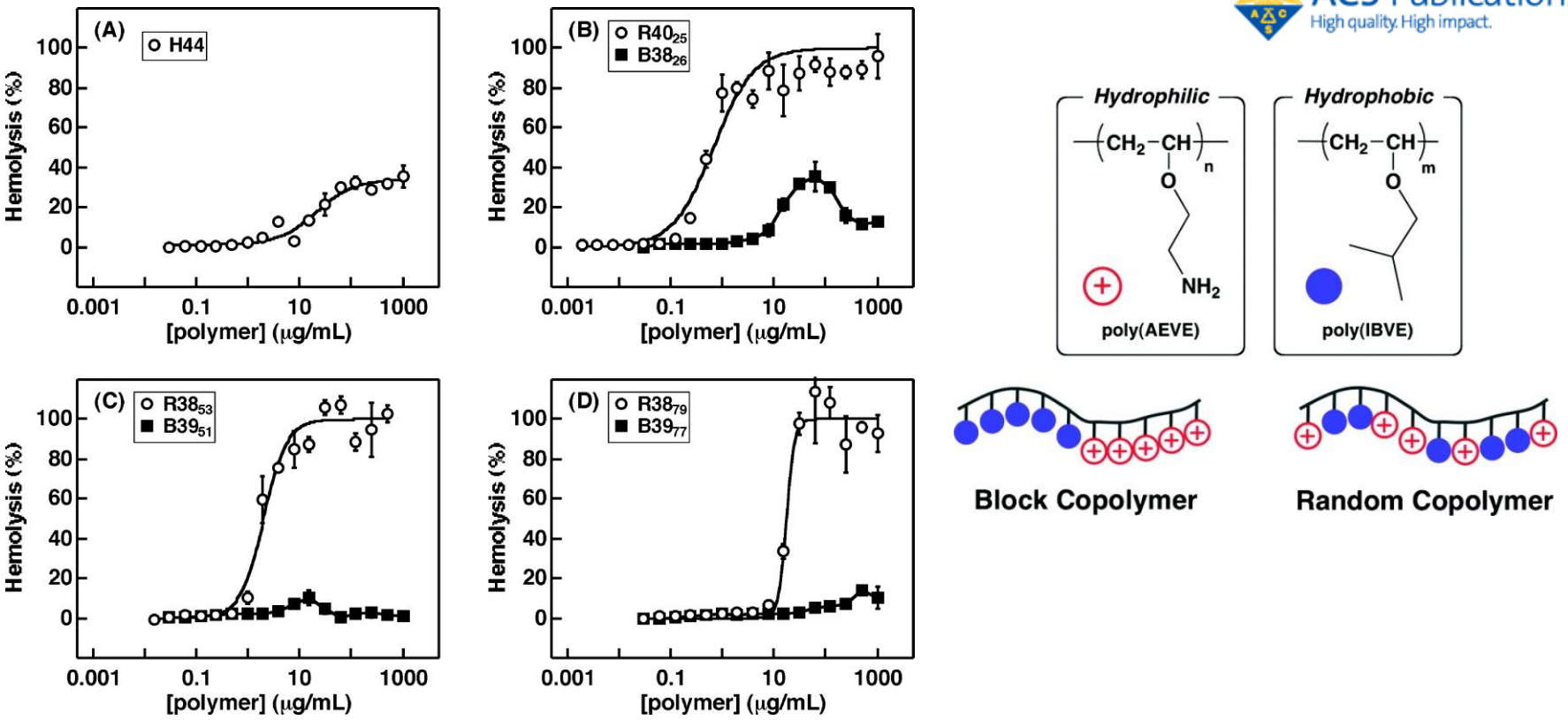


Percentages of hemolysis induced by homopolymer (A), copolymers with MPIBVE = ~25% (B), 50% (C), and 80% (D). The data points and error bars represent the average and standard deviations of a representative measurement in triplicate. The sigmoidal curves of homopolymer (A) and random copolymers (B–D) are best fits to the Hill equation.

The HC50 values of the random copolymers increased with increasing MPIBVE, indicating that increasing the hydrophobicity of polymers reduces the hemolytic activity. However, random amphiphilic polymethacrylates with high mole percentages of hydrophobic side chains showed high hemolytic activity,(11, 15) which is opposite to the results presented in this study. As discussed for the antibacterial activity of polymers, the random poly(vinyl ether)s with higher MPIBVE could form intramolecular aggregates due to the flexible polymer backbone, which reduces the active polymer chains, resulting in the lower hemolytic activity.

Published in: Yukari Oda; Shokyoku Kanaoka; Takahiro Sato; Sadahito Aoshima; Kenichi Kuroda; *Biomacromolecules* **2011,** 12, 3581-3591.
DOI: 10.1021/bm200780r

# able 2. Bactericidal Activity and Hemocompatibility of the Copolymers

| polymer | $BC_{99.9}$[a] (μg/mL) in HEPES | $BC_{99.9}$[a] (μg/mL) in MH broth | $HC_{50}$[b] (μg/mL) | $C_H$[d] (μg/mL) |
|---|---|---|---|---|
| H44 | 1.6 ± 0.0 | 54.7 ± 15.6 | >1000 (max 42.5 ± 6.3%)[c] | 0.98 |
| $R40_{25}$ | 1.6 ± 0.0 | 15.6 ± 0.0 | 0.49 ± 0.17 | >1000 |
| $R38_{53}$ | 3.1 ± 0.0 | 62.5 ± 0.0 | 1.8 ± 0.24 | >500 |
| $R38_{79}$ | 31.3 ± 0.0 | 1000 ± 0.0 | 18.9 ± 1.3 | >1000 |
| $B38_{26}$ | 2.4 ± 0.91 | 62.5 ± 0.0 | >1000 (max 37.7 ± 2.8%)[c] | 2.0 |
| $B39_{51}$ | 3.1 ± 0.0 | 250 ± 0.0 | >1000 (max 12.9 ± 6.3%)[c] | 0.49 |
| $B39_{77}$ | 62.5 ± 0.0 | >1000 | >1000 (max 22.8 ± 8.5%)[c] | 0.78 |

a Determined in HEPES buffer or MH broth against *E. coli*.
b The $HC_{50}$ values and errors were reported as average and standard deviations of the three independent experiments, respectively.
c Local maximum values of hemolysis induced by each polymer.
d The lowest polymer concentration to induce hemagglutination.

Gibco HEPES (4-(2-hydroxyethyl)-1-piperazineethanesulfonic acid ) is a zwitterionic organic chemical buffering agent and is categorized as a "Good" buffer which derives from a set of buffers described by Dr. Norman Good and his colleagues in 1966 (Good *et. al.*, Biochemistry 1966). "Good buffers" such as HEPES are attributed with the following characteristics:

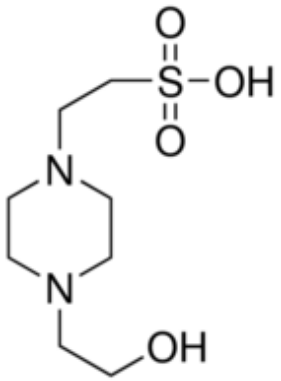


pKa values between 6.0 and 8.0
high solubility
membrane impermeability
limited effect on biochemical reactions
very low visible and ultraviolet light absorbance
chemically and enzymatically stable
easy to prepare.

1M in water

HEPES is widely used in many biochemical reactions and as a buffering agent in some cell culture media.

**General description-Aldrich**

HEPES has been described as one of the best all-purpose buffers available for biological research.[7] At biological pH, the molecule is zwitterionic, and is effective as a buffer at pH 6.8 to 8.2. HEPES has been used in a wide variety of applications, including tissue culture. It is commonly used to buffer cell culture media in air. HEPES finds its usage in *in vitro* experiments on Mg.[1]

# 70192 Mueller Hinton Broth (M-H Broth)

A liquid medium for antibiotic susceptibility studies (MIC-determination).

**Composition:**

| Ingredients | Grams/Litre |
|---|---|
| Beef infusion solids | 2.0 |
| Starch | 1.5 |
| Casein hydrolysate | 17.5 |
| Final pH 7.4 +/- 0.2 at 25°C | |

Store prepared media below 8°C, protected from direct light. Store dehydrated powder, in a dry place, in tightly-sealed containers at 2-25°C.

**Directions :**
Dissolve 21 g in 1 litre of distilled water. Sterilize by autoclaving at 121°C for 15 minutes.

**Principle and Interpretation:**
Mueller Hinton Broth is used for determining minimal inhibitory concentrations (MICs). Mueller Hinton medium is recommended by FDA, World Health Organization and NCCLS for testing most commonly encountered aerobic and facultative anaerobic bacteria in food and clinical material. The medium shows good batch-to-batch reproducibility, it is low in sulfonamide, trimethoprim, and tetracycline inhibitors and yields satisfactory growth of most non-fastidious pathogens.
Beef infusion and Casein provide nitrogenous compounds, vitamins, carbon, sulphur and amino acids in Mueller Hinton media. Starch is added to absorb any toxic metabolites produced.
For testing streptococci, supplementation with 5% defibrinated sheep or horse blood is recommended. Mueller Hinton media should be supplemented with 2% NaCl for testing methicillin or oxacillin (28221) against staphylococci. Mueller Hinton media with Rabbit Serum is used for the susceptibility of microorganisms to sulfonamides and trimethoprim. Antagonism to sulfonamide activity is demonstrated by para-aminobenzoic acid
(PABA) and its analogs. Reduced activity of trimethoprim is demonstrated on medium possessing high levels of thymidine. The PABA and thymine/thymidine content of Mueller Hinton media is reduced to a minimum.

Cultural characteristics after 24 hours at 35°C.

| Organisms (ATCC) | Growth |
|---|---|
| *Escherichia coli* (25922) | +++ |
| *Staphylococcus aureus* (25923) | +++ |
| *Pseudomonas aeruginosa* (27853) | +++ |
| *Neisseria meningitidis* (13090) | +++ |
| *Streptococcus faecalis* (29212) | +++ |

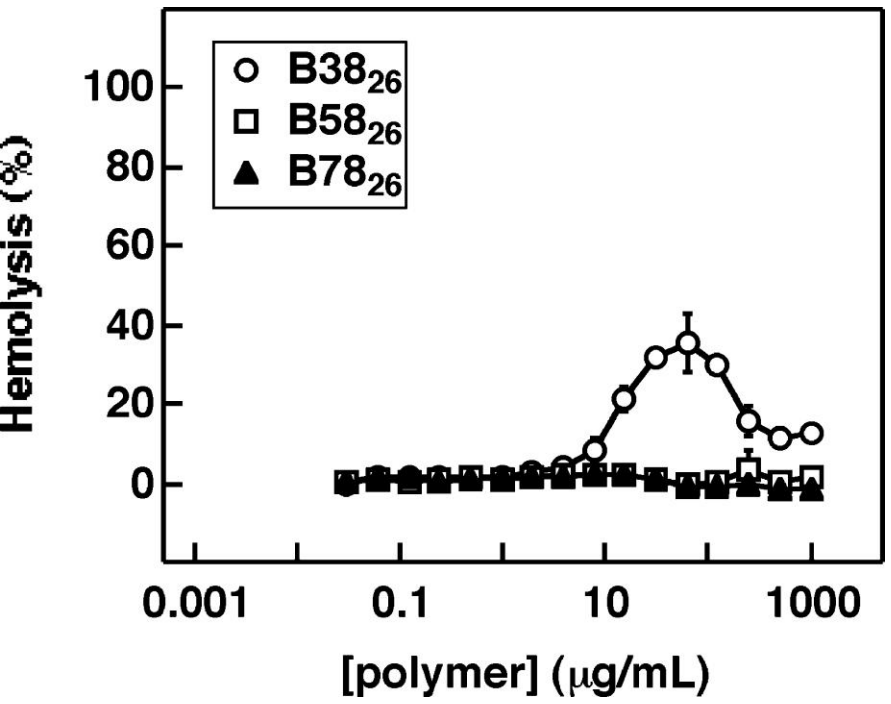


Table 3. Effect of Polymer Length on Bactericidal Activity of Block Copolym

| | $BC_{99.9}$[a] | | | |
|---|---|---|---|---|
| | in HEPES | | in MH broth | |
| polymer | (μg/mL) | (μM) | (μg/mL) | (μM) |
| $B38_{26}$ | 2.4 | 0.66 | 62.5 | 17.5 |
| $B58_{26}$ | 0.78 | 0.15 | 62.5 | 11.9 |
| $B78_{26}$ | 1.6 | 0.22 | 31.3 | 4.4 |

a Determined in HEPES buffer or MH broth against *E. coli*.

Percentages of hemolysis induced by B3826 (empty circles), B5826 (empty squares), and B7826 (filled triangles) as a function of polymer concentration. Error bars represent the standard deviations from triplicate measurements. B3826 caused a local maximum of 30% hemolysis at 100 μg/mL, but the block polymers with increased DP, B5826, and B7826, induced no hemolysis up to 1000 μg/mL. This indicates that the hemolytic activity of the block copolymers was reduced by increasing the DP.

Published in: Yukari Oda; Shokyoku Kanaoka; Takahiro Sato; Sadahito Aoshima; Kenichi Kuroda; *Biomacromolecules* **2011,** 12, 3581-3591.
DOI: 10.1021/bm200780r

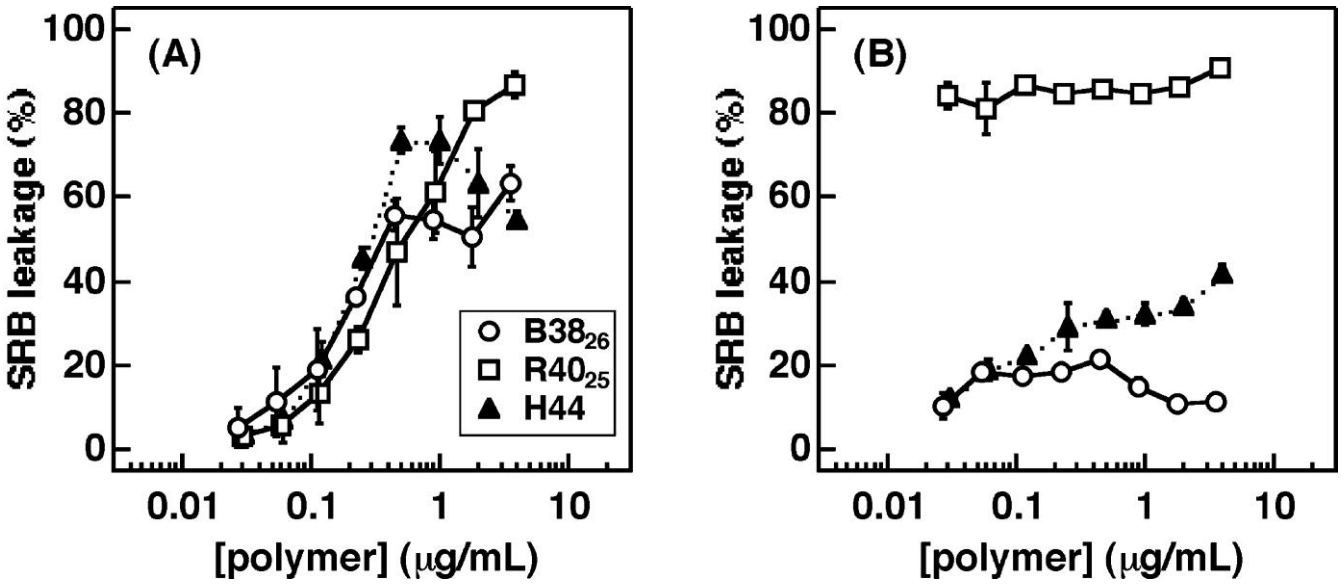


Percentages of SRB leakage from LUVs composed of (A) POPE/POPG (4:1) and (B) eggPC. The LUVs were incubated with the polymers B3826 (empty circles), R4025 (empty squares), and H44 (filled triangles) at 37 ° C for 1 h. The error bars represent the standard deviations from triplicate measurement.

LUVs with POPE/POPG (4:1) and eggPC are simplified model membranes of the *E. coli* and RBC cell membranes, respectively. These model vesicles are limited by their lipid compositions, as the bacterial cell and RBC membranes are a complex of proteins, lipids, and polysaccharides on the cell surface with membrane asymmetry. The leakage from eggPC LUVs depended on the amphiphilic copolymer structures (Figure 5B). The leakage induced by the block copolymer $B38_{26}$ was lower than 20% although the random copolymer $R40_{25}$ induced >80% leakage in the entire concentration range (0.029–3.8 μg/mL). These results suggest that the block copolymer selectively disrupts the bacteria-type membranes over the erythrocyte-type membranes, which appears to reflect the selective activity of polymers against *E. coli* over RBCs although the antibacterial actions of polymers remain unclear.

Published in: Yukari Oda; Shokyoku Kanaoka; Takahiro Sato; Sadahito Aoshima; Kenichi Kuroda; *Biomacromolecules* **2011,** 12, 3581-3591.
DOI: 10.1021/bm200780r

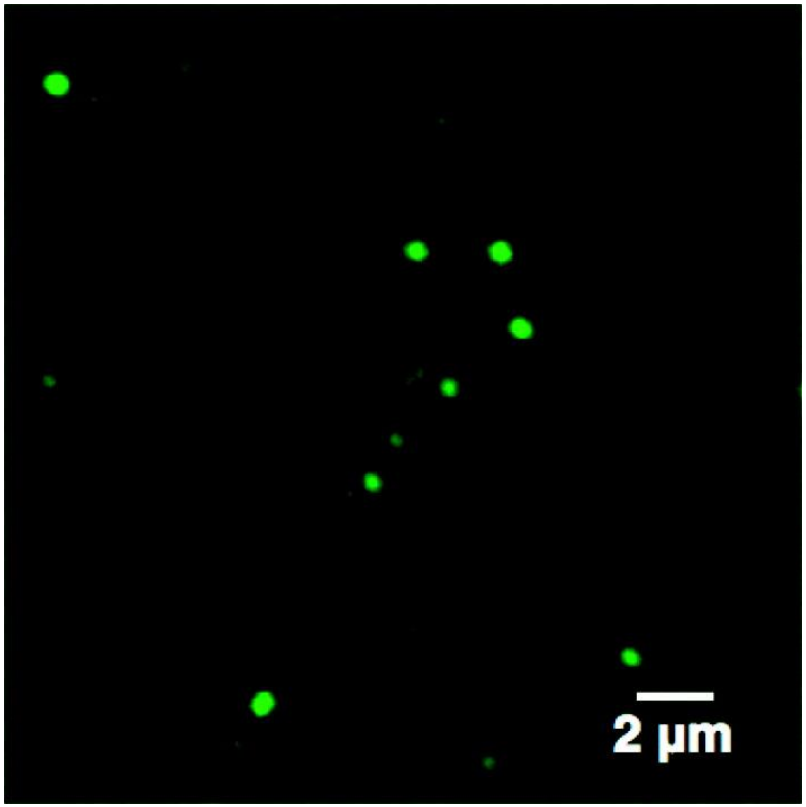


Confocal fluorescent microscopy image (single layer image) of 50 µg/mL B3826 containing F-B3826 in HEPES buffer (1% v/v DMSO; FITC: 5.3 mol % relative to the total number (mole) of B3826 polymer chains).

Published in: Yukari Oda; Shokyoku Kanaoka; Takahiro Sato; Sadahito Aoshima; Kenichi Kuroda; *Biomacromolecules* **2011,** 12, 3581-3591.
DOI: 10.1021/bm200780r

# Table 4. Characterization of Polymer Aggregates in HEPES Buffer

| polymer | $S^2_{z}^{1/2}$ [a] (nm) | $R_H$ [b] (nm) | $M_w$ [c] | $N_{agg}$ [d] | CAC [e] (μg/mL) | $BC_{99.9}$ [f] (μg/mL) | $HC_{50}$ (μg/mL) |
|---|---|---|---|---|---|---|---|
| B38<sub>26</sub> | 200 | 250 | $8.1 \times 10^7$ | 20000 | 36 | 2.4 ± 0.91 | >1000 |
| R40<sub>25</sub> | 27 | n.d. [g] | $9.4 \times 10^4$ | 22 | 380 | 1.6 ± 0.0 | 0.49 ± 0.17 |

a Radius of gyration, determined by SLS.
b Hydrodynamic radius, determined by DLS.
c Weight-average molecular mass, determined by SLS.
d Aggregation number, calculated from the weight-average molecular weight of polymer chain and $M_w$.
e Critical (intermolecular) aggregation concentration, determined by SLS.
f Determined in HEPES buffer.
g The scattering intensities were too low to obtain accurate autocorrelation functions.

3. Determination of the critical (intermolecular) aggregation concentration (CAC)

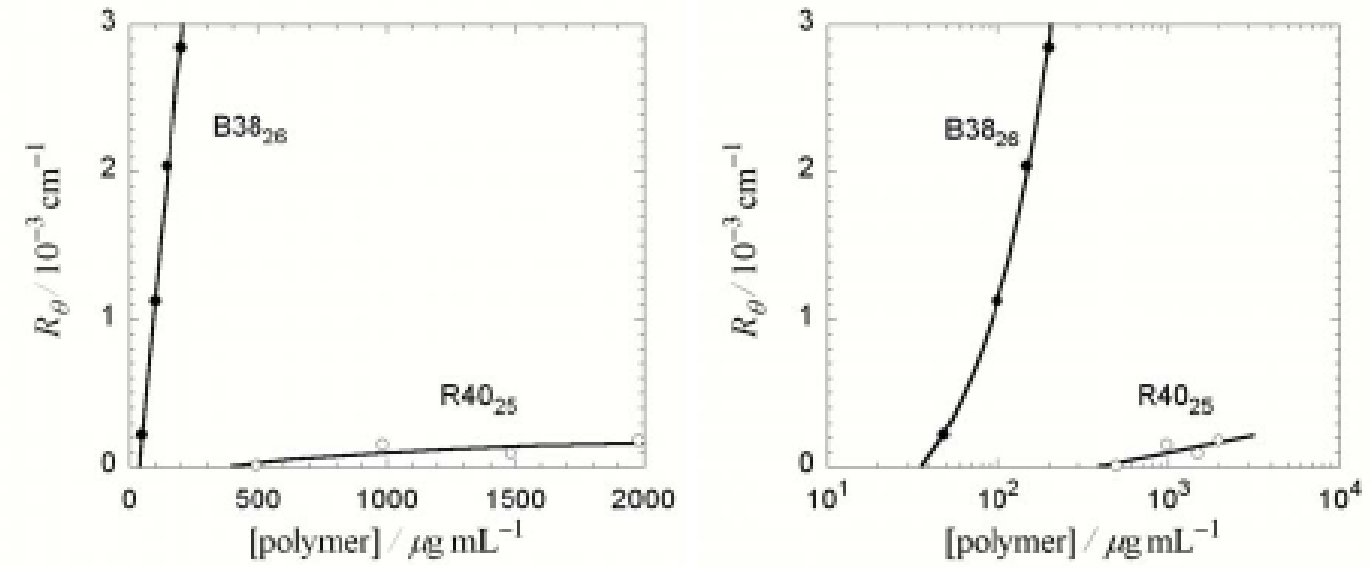


**Figure S7.** Linear (left) and semi-logarithmic (right) plots of the excess Rayleigh ratio against the polymer concentration for aqueous solutions of samples $B38_{26}$ and $R40_{25}$.

The critical (intermolecular) aggregation concentration (CAC) was determined as the polymer concentration where the excess Rayleigh ratio $R_\theta$ becomes infinitely low. Figure S7 shows the polymer concentration dependence of $R_\theta$ at $\theta = 30°$ for aqueous solutions of samples $B38_{26}$ and $R40_{25}$, from which CAC were determined to be 36 μg/mL and 380 μg/mL for $B38_{26}$ and $R40_{25}$, respectively.

4. Static and dynamic light scattering data

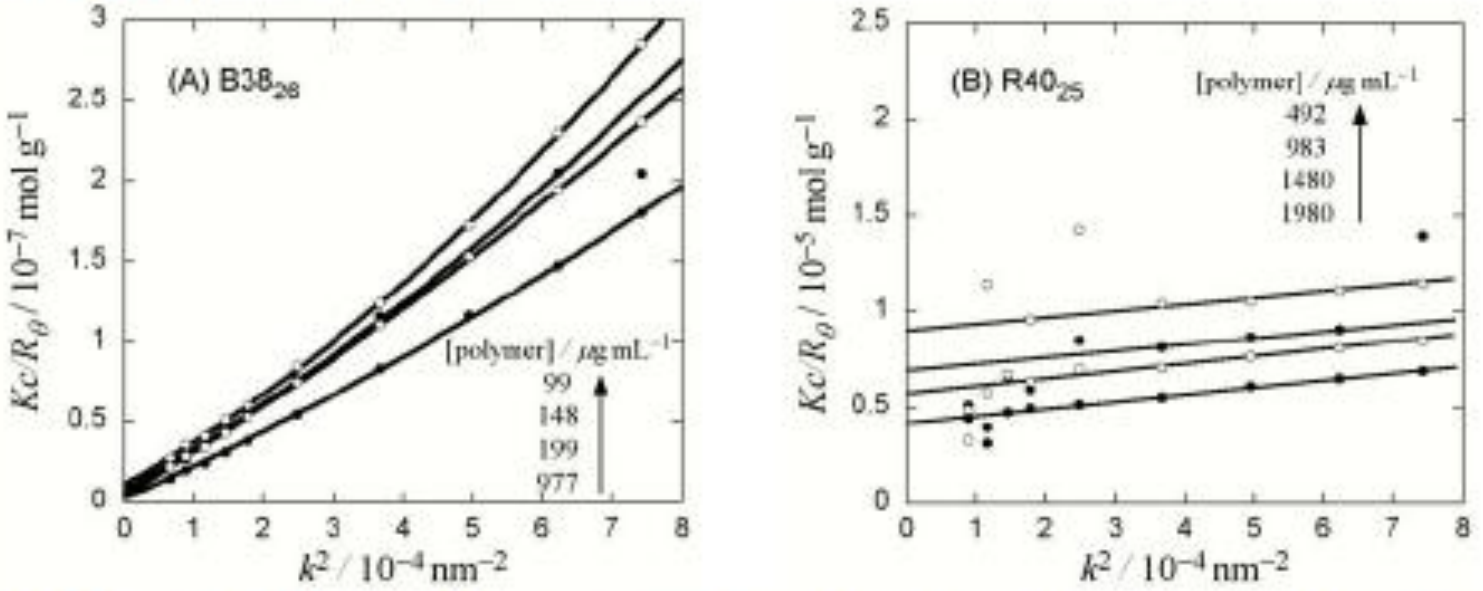


Figure S8. Static light scattering (SLS) results for B38$_{26}$ (A) and R40$_{25}$ (B) in HEPES buffer at 37 °C.

The hydrodynamic radius of the block copolymer aggregate obtained by DLS was as large as 250 nm. The aggregate sizes estimated by the light scattering experiments are consistent with those found in the fluorescence image. On the other hand, light scattering intensities from aqueous solutions of the random copolymer R4025 were much weaker than B3826 solutions, and the radius of gyration and the aggregation number were 27 nm and 22, respectively, in the copolymer concentration range 500–2000 μg/mL

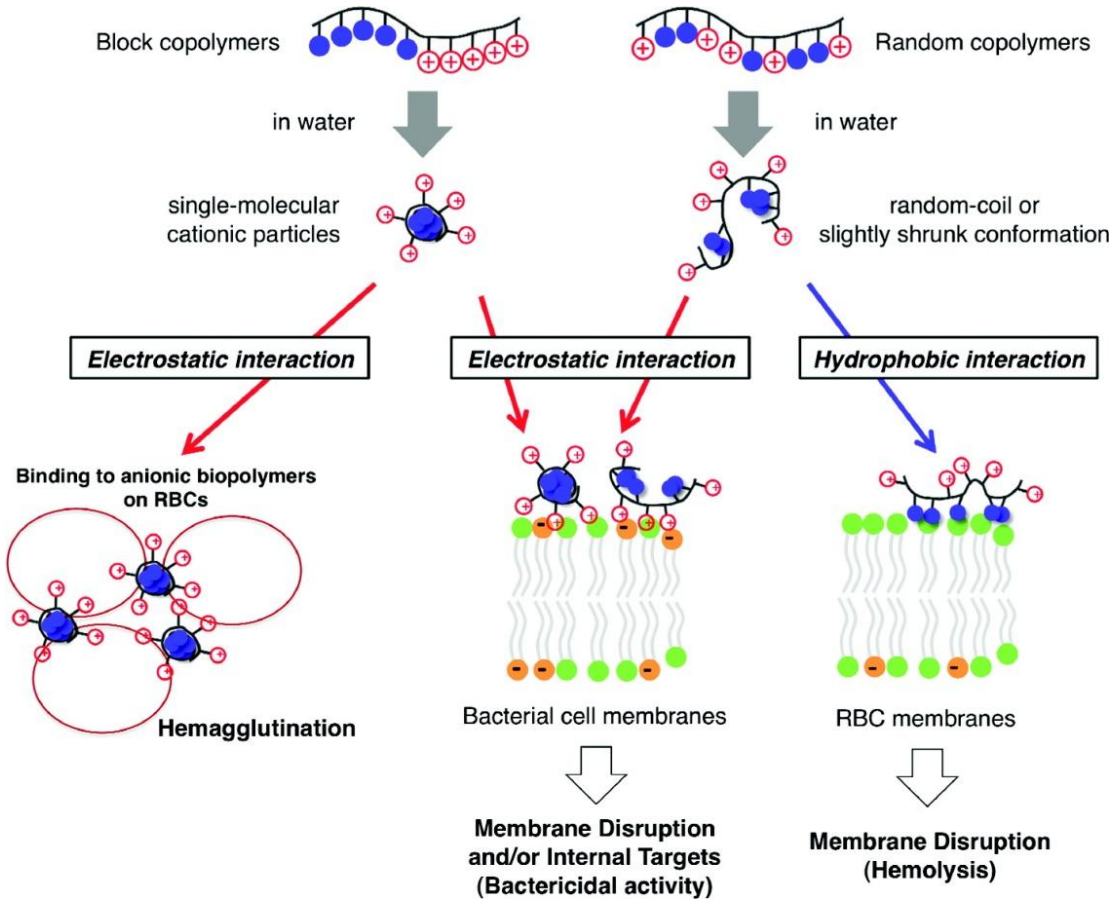


However, the high cationic charge density of the intramolecular aggregates could interact strongly with the anionic biopolymers on the RBC surfaces, which cause hemagglutination. **Hemagglutination**, or **haemagglutination**, is a specific form of agglutination (clumping of the particles) that involves red blood cells (RBCs). The virus will also bind to erythrocytes (red blood cells), causing the formation of a lattice. This property is called hemagglutination, and is the basis of a rapid assay to determine levels of influenza virus present in a sample.

Schematic presentation of proposed antibacterial and hemolytic activities.

Published in: Yukari Oda; Shokyoku Kanaoka; Takahiro Sato; Sadahito Aoshima; Kenichi Kuroda; *Biomacromolecules* **2011,** 12, 3581-3591.
DOI: 10.1021/bm200780r

The block copolymers could form intramolecular aggregates with a hydrophobic core wrapped by the cationic segment in water, which can be regarded as single-molecular cationic particles. The cationic properties of these intramolecular aggregates would increase their electrostatic binding to anionic lipopolysaccharides (LPS) on the *E. coli* cell surface and may replace the divalent cations, which stabilize the outer membrane structure. The replacement of these divalent cations destabilizes the membrane structure and increases permeability of the outer membrane, which would promote uptake of the polymers into the cell surfaces as found in antimicrobial peptides. The polymers could diffuse through the peptidoglycan layer to reach cytoplasmic membranes with anionic lipids and cause membrane disruption, leading to lethal leakage of cellular contents. The cationic groups of polymers could induce the segregation of anionic lipids or cause strong perturbation of the cell wall integrity.Alternatively, the polymers might transit the cytoplasmic membrane and interact with potential targets in the cytoplasma, inhibiting macromolecular synthesis as found for some antimicrobial peptides. As for the hemolytic activity, the hydrophobic segment is shielded by the cationic surfaces, reducing the hydrophobic binding of polymers to the cell membranes of RBCs, thus, causing no significant hemolytic activity. However, the high cationic charge density of the intramolecular aggregates could interact strongly with the anionic biopolymers on the RBC surfaces, which cause hemagglutination. On the other hand, random copolymers would take a random-coil or slightly shrunk conformation because the hydrophobic groups randomly distributed along the polymer chain may not form the hydrophobic core (Figure 7), if the hydrophobic content is low enough

**Polymeric coatings that inactivate both influenza virus and pathogenic bacteria**

**Jayanta Haldar*, Deqiang An*, Luis A´ lvarez de Cienfuegos*, Jianzhu Chen†‡, and Alexander M. Klibanov*, ¶**

PNAS **November 21, 2006 vol. 103 no. 47 17667–17671**

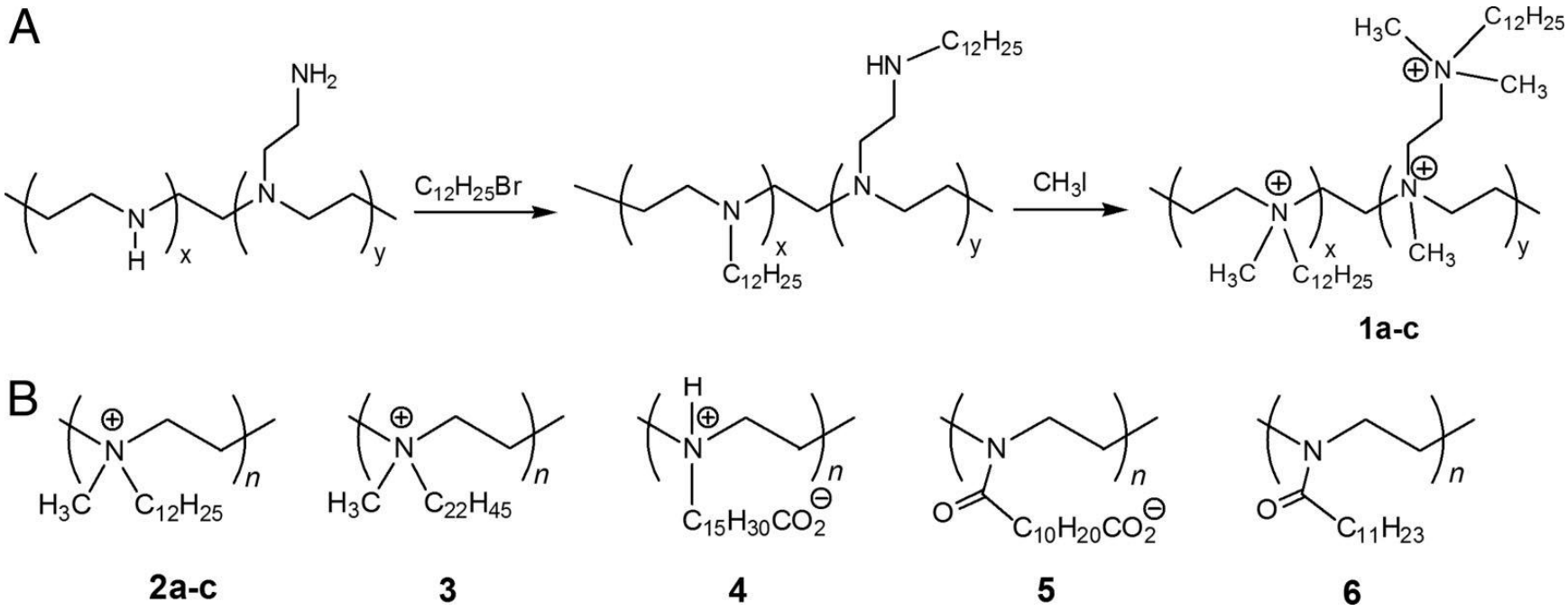


**Fig. 1. Hydrophobic PEI derivatives prepared in the study. (*A) Schematic representation of the N-dodecylation and subsequent N-methylation of branched PEIs*** (see *Materials and Methods for details). In the case of **1, the letters a, b, and c correspond to the N,N-dodecyl methyl-polycations prepared from 750-, 25-, and** 2-kDa PEIs, respectively. (*B) Chemical structures of linear PEI-based polymers synthesized in this work. In the case of **2, the letters a, b, and c correspond to the** N,N-dodecyl methyl-polycations prepared from 217-, 21.7-, and 2.17-kDa PEIs, respectively. For **3 through 6, 217-kDa PEI was used.***

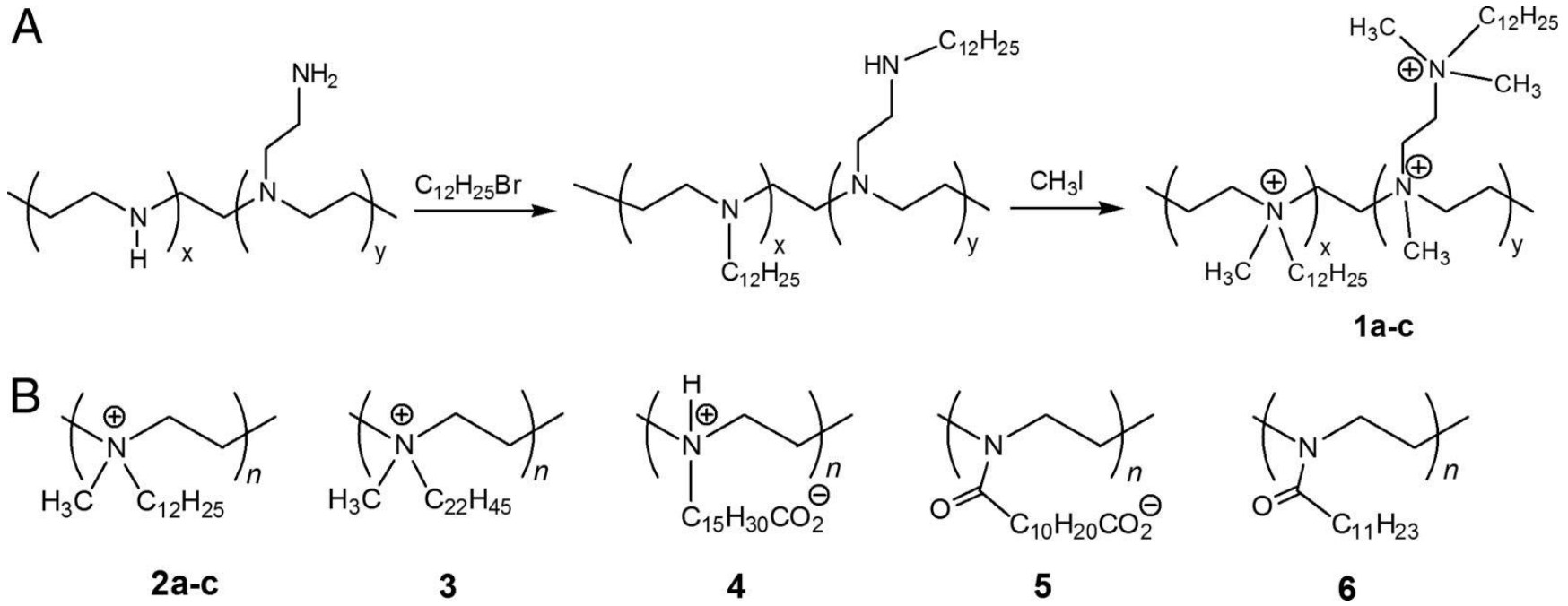


A 10-l droplet of a PBS-buffered solution containing (1.6 ±0.3) $10^3$ pfu of the AWSN33 (H1N1) strain of influenza virus was placed in the center of a 2.5 x 2.5 cm glass slide (either coated or plain control).

*N,N-dodecyl methyl-PEI (**1a) (synthesized by quaternizing a*** branched 750-kDa PEI as depicted in Fig. 1) in butanol and let the solvent evaporate.

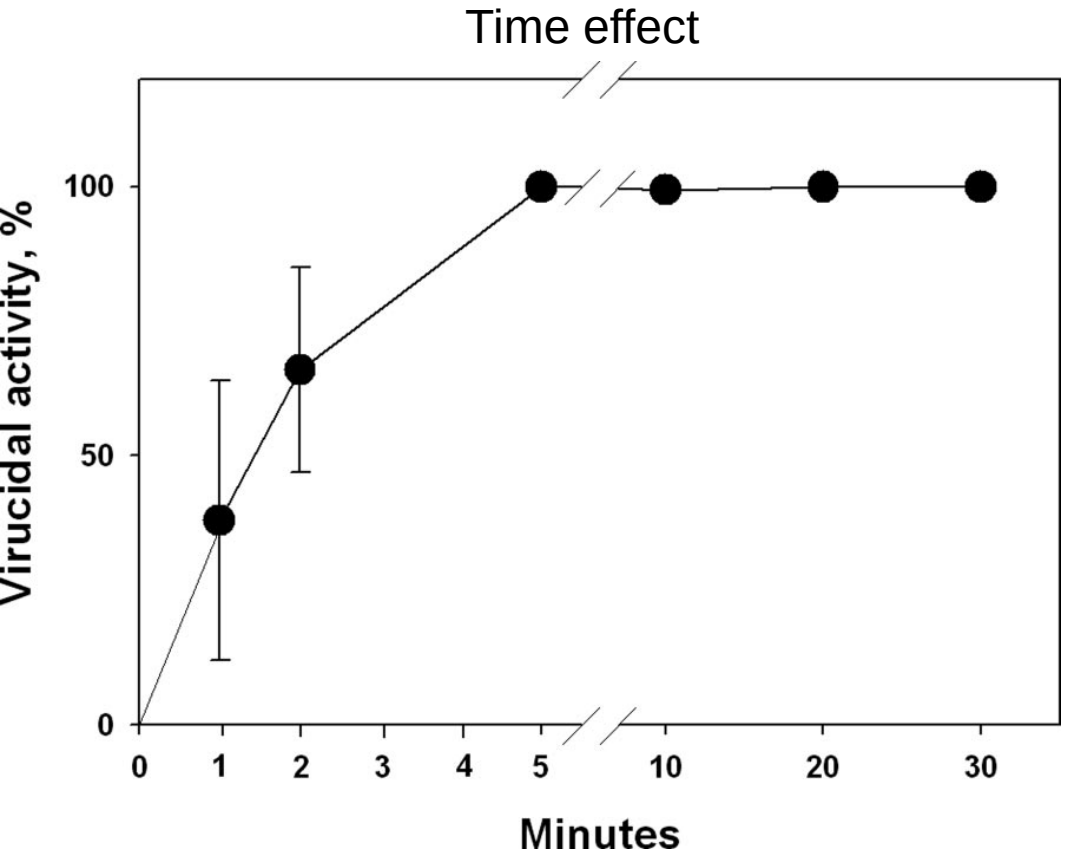


**Fig. 2. The time course of inactivation of influenza virus (WSN strain) by a** glass slide painted with **2a at r.t. See *Materials and Methods for details.***

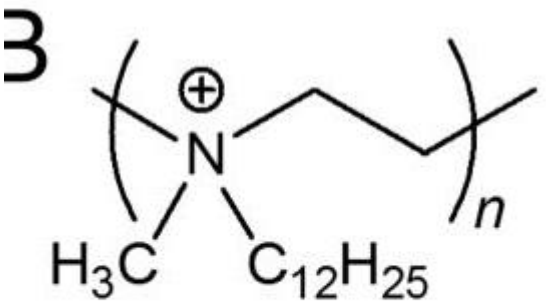


**2a-c**

**2a, 2b, and 2c, synthesized from the 217-kDa, 21.7-kDa, and 2.17-** kDa linear PEI precursors, respectively. Slides coated with all of these linear hydrophobic polycations indeed inactivated influenza virus with a 100% efficiency. Moreover, **2a (like 1a) was** shown to reduce the viral titer by at least some 4 logs; it was used in most subsequent experiments.

**Table 1. Microbicidal activity of glass slides painted with 1a, 2a, 4, 5, and 6**

| PEI derivative | Virucidal activity* after 30 min, % | Bactericidal activity, % | |
|---|---|---|---|
| | | *S. aureus* | *E. coli* |
| 1a | 100 | 99 ± 1 | 99 ± 1 |
| 2a | 100 | 100 | 100 |
| 4 | 100 | 26 ± 4 | 14 ± 2 |
| 5 | 66 ± 3 | 21 ± 1 | 22 ± 3 |
| 6 | 6 ± 6 | 34 ± 1 | 14 ± 2 |

Glass slides used in these experiments were painted twice or more to attain the levels of activity indicated (presumably reflecting imperfections of our painting procedure).
*Virucidal activities were tested against the WSN strain of influenza virus.

When the PEI precursors of **1 with molecular masses of lower** than 750 kDa, namely 25 kDa and 2 kDa, were used to make the hydrophobic polycationic coatings (**1b and 1c, respectively), still** very high but slightly incomplete virucidal efficiencies were observed, 98  0.4% and 97  0.2%, respectively.

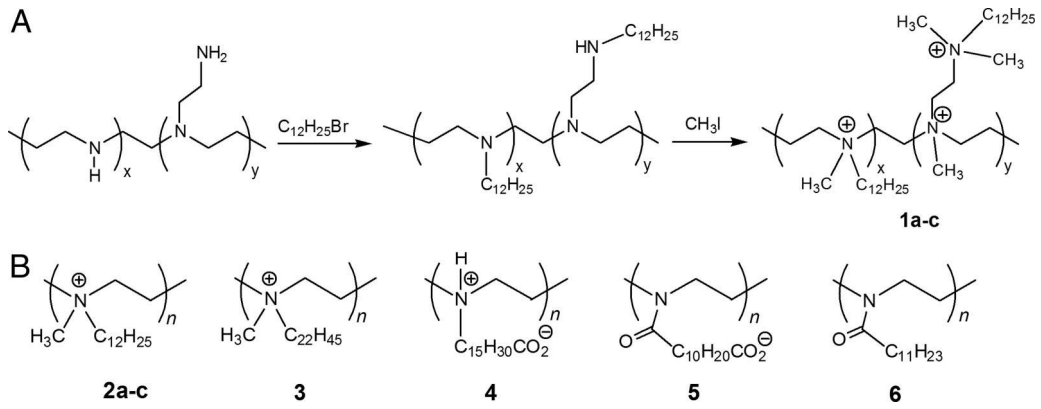


To ascertain the role of the charge, we also synthesized derivatives of linear 217-kDa PEI that were nominally zwitter-ionic (**4), anionic (5), and electrostatically neutral (6) with otherwise** roughly similar side chains as in **1 and 2 (Fig. 1). As shown in the** second column of Table 1, zwitter-ionic **4, just as cationic 1a and 2a (and also 2b–c and 3, see above), is 100% virucidal after a** 30-min exposure. In contrast, the anionic **5 is only partially** virucidal, and the neutral **6 is not virucidal at all.**

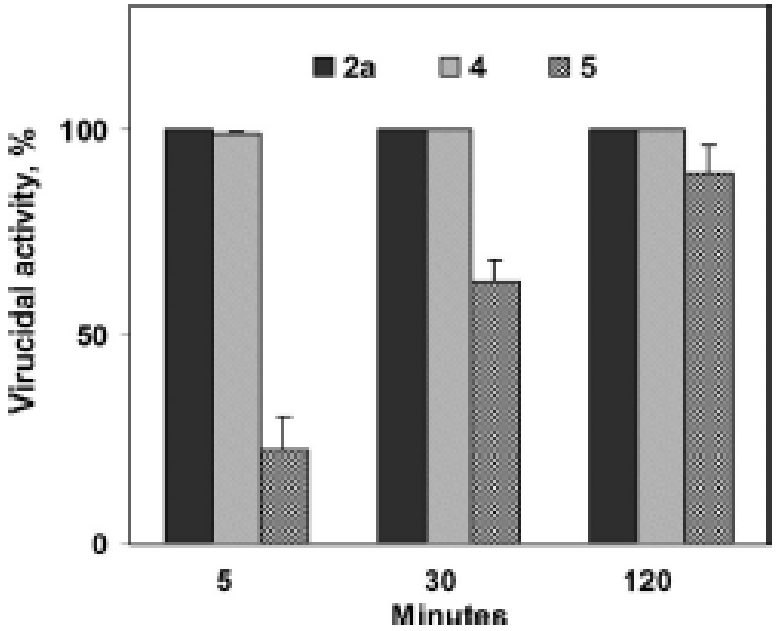


Fig. 3. The virucidal activity against influenza virus (WSN strain) of glass slides painted with 2a, 4, and 5 after different times of exposure at r.t. See *Materials and Methods* for details.

To gain further insights into these observations, we investigated the time course of the virucidal activity of slides coated with **4 and 5. Not only did zwitter-ionic 4, like cationic 2a, already** inactivate the entirety of the exposed influenza virus after a 30-min incubation, but even after just 5 min the virucidal activity of **4 was as high as 98  0.7% (Fig. 3). Interestingly, the virucidal** activity of anionic **5 rose steadily with time (see the last bar at** each time point in Fig. 3) to reach 89  7% after a 2-h exposure. Thus, it seems that the differences in virucidal activities among the polymeric coatings are a matter of kinetics rather than ultimate degree, i.e., that the hydrophobic polycations merely inactivate the virus faster than other hydrophobic polyions.

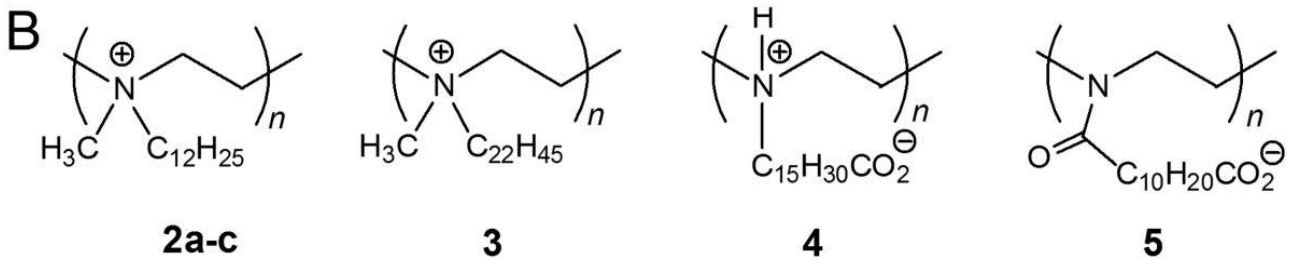

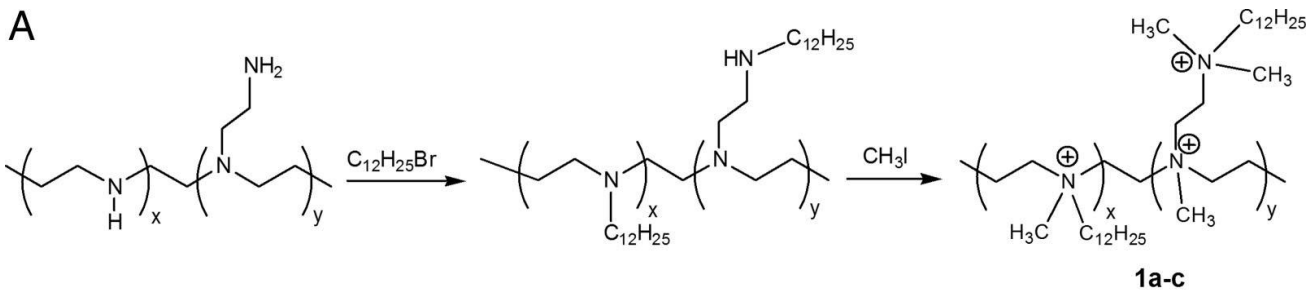


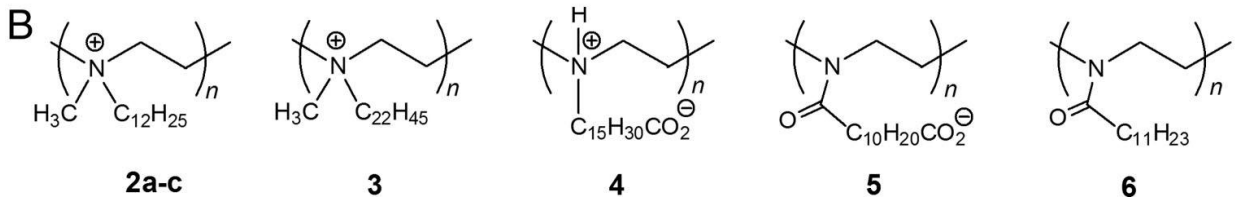


POLYMER → LEACH OUT?-two test were applied.

On the basis of the results of the foregoing controls, we conclude that, at least for slides painted with **1a, 1b, 2b, 3, 4, and 5, the virucidal activity observed is attributable solely to the** polyions remaining deposited on the slide's surface, i.e., the tentacles of these immobilized polyions inactivate the virus on contact. In contrast, in the case of **1c, 2a, and 2c coatings,** contributions of the leached polycations to the virucidal activity of the painted slides cannot be ruled out.

**Zanamivir Conjugated to Poly-L-Glutamine is Much More Active Against Influenza Viruses in Mice and Ferrets Than the Drug Itself**

Alisha K. Weight & Jessica A. Belser & Terrence M. Tumpey & Jianzhu Chen & Alexander M. Klibanov, Pharm Res (2014) 31:466–474

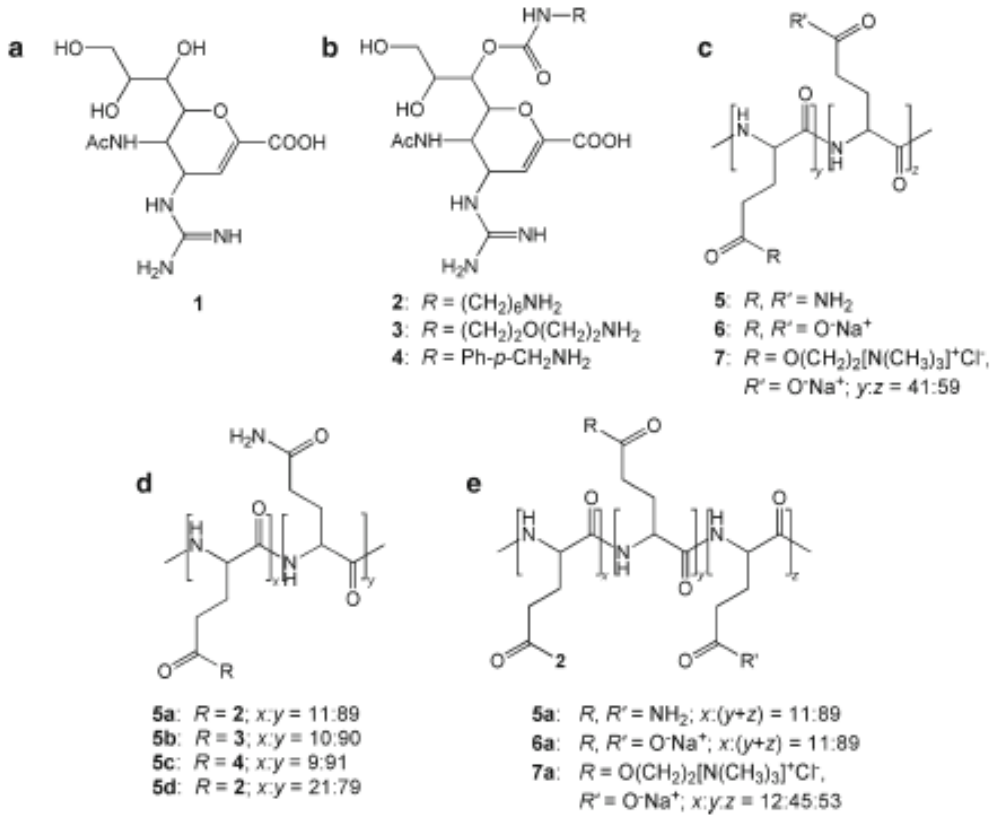


**Fig. 1** Chemical structures (**a**) of zanamivir itself (**1**) and (**b**) of its derivatives with different linkers (**2**–**4**) for attachment to (**c**) polymer scaffolds with different electrostatic charges (neutral, negative, and zwitter-ionic) (**5**–**7**) to give polymer conjugates with (**d**) varying linker groups (**5a**–**5c**) and (**e**) charges on the polymer backbone (**5a**–**7a**).

**Results** 1 attached to poly-L-glutamine is an effective therapeutic for established influenza infection in ferrets, reducing viral titers up to 30-fold for 6 days. There is also up to a 190-fold reduction in viral load when the drug is used as a combined prophylactic/therapeutic in mice. Additionally, we see no evidence that the drug conjugate stimulates an immune response in mice upon repeat administration.

(i) a rigid hydrophobic phenyl moiety and (ii) a flexible and hydrophilic ethylene glycol moiety (Fig. 1b, compounds 3 and 4, respectively).

| | |
|---|---|
| Nanchang | influenza strain A/Nanchang/933/95 |
| p.i. | post-infection |
| PR8 | influenza strain A/PR/8/34 |
| SAR | structure-activity relationship |
| TKY | influenza strain A/turkey/MN/833/80 |
| TKY E119D | influenza strain A/turkey/MN/833/80/E119D |
| WSN | influenza strain A/WSN/33 |
| Wuhan | influenza strain A/Wuhan/359/95 |

Within 10 min, mice were then infected with 25 μL of a virus solution in PBS (1,000 pfu/mouse) delivered in the same nostril. At 6, 24, and 48 h postinfection (p.i.), mice were again given PBS, 1, 5, or 5a.

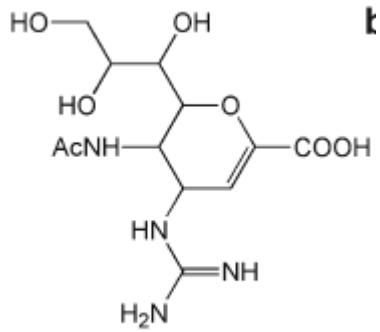


1

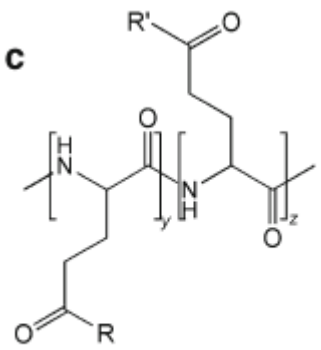


**5**: $R, R' = NH_2$

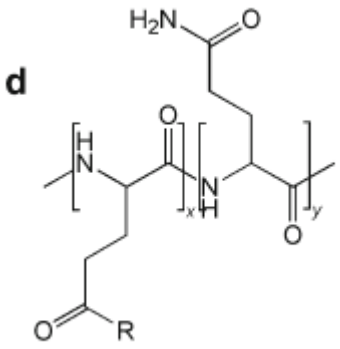


**5a**: $R$ = **2**; $x$:$y$ = 11:89

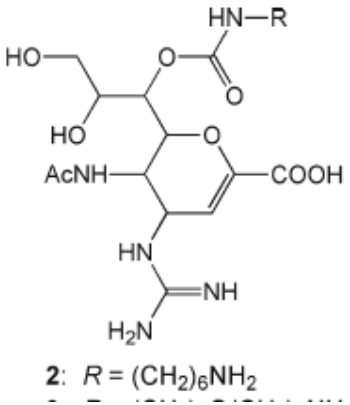


**2**: $R = (CH_2)_6NH_2$

**Table I** Antiviral Activities of **1**'s Analogs **2**–**4** and Their High-Molecular-Weight-Polymer-Attached Derivatives **5a**-**5c** Against Three Strains of Influenza A Virus, as Determined by the Plaque Reduction Assay

| Inhibitor | $IC_{50}$ (nM **1**)[a] | | |
|---|---|---|---|
| | WSN | Wuhan[b] | TKY[b] |
| **2** | $(1.0 \pm 0.4) \times 10^4$ | $(4.3 \pm 0.20) \times 10^5$ | $(4.3 \pm 1.1) \times 10^4$ |
| **3** | $(5.7 \pm 3.9) \times 10^4$ | $(1.3 \pm 0.56) \times 10^6$ | $(1.4 \pm 0.34) \times 10^6$ |
| **4** | $(7.6 \pm 1.3) \times 10^4$ | $(8.4 \pm 1.3) \times 10^5$ | $(2.3 \pm 0.71) \times 10^6$ |
| **5a** | $(1.8 \pm 0.5) \times 10^2$ | $21 \pm 7.3$ | $(1.8 \pm 0.20) \times 10^2$ |
| **5b** | $(1.3 \pm 0.80) \times 10^2$ | $(1.5 \pm 0.63) \times 10^2$ | $(1.5 \pm 0.70) \times 10^3$ |
| **5c** | $81 \pm 1.0$ | $43 \pm 23$ | $(9.8 \pm 1.2) \times 10^3$ |

[a] Reported values were determined from experiments run at least in triplicate. The $IC_{50}$ values (± SD) are expressed as nanomolar concentrations of **1**, whether free or conjugated to poly-*L*-glutamine. To determine the $IC_{50}$ values, inhibitor and influenza viruses were incubated together prior to the plaque assay. Therefore, the $IC_{50}$ values reflect inhibition of infection. The $IC_{50}$ values for unmodified poly-*L*-glutamine ranged from 2 to 14 mM (on a monomer basis), indicating that the polymer itself had no appreciable antiviral activity

[b] The $IC_{50}$ values for compounds **2** and **5a** against Wuhan and TKY strains, previously reported by us (12), are included here for comparison

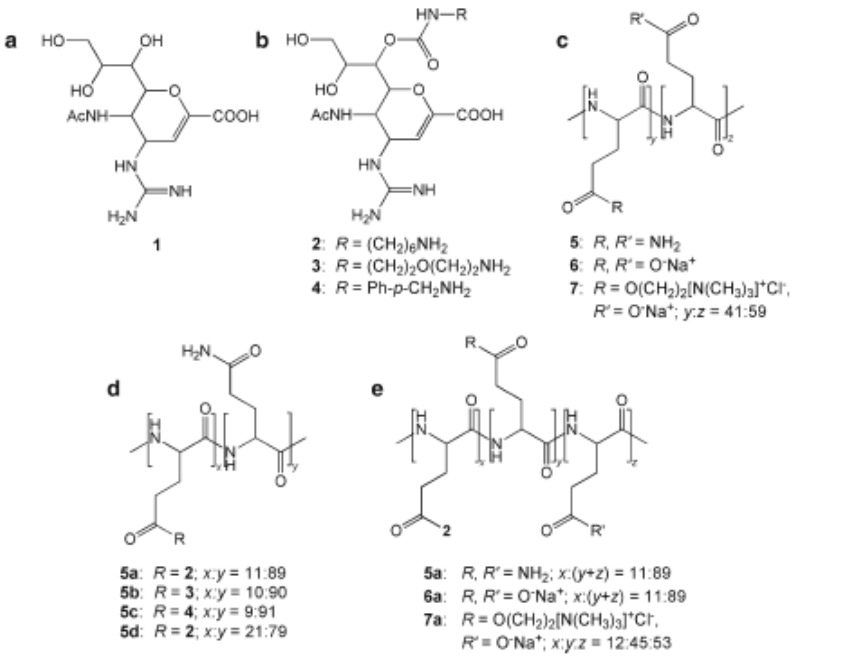


**Fig. 1** Chemical structures (**a**) of zanamivir itself (**1**) and (**b**) of its derivatives with different linkers (**2**-**4**) for attachment to (**c**) polymer scaffolds with different electrostatic charges (neutral, negative, and zwitter-ionic) (**5**–**7**) to give polymer conjugates with (**d**) varying linker groups (**5a**-**5c**) and (**e**) charges on the polymer backbone (**5a**-**7a**).

Poly-L-glutamine-attached zanamivir 5a (Fig. 1a) is a far more potent inhibitor of influenza A virus than 1 itself due to the multivalency effect (9,12). For all three strains, IC50 (half of maximal inhibitory concentration) values showed that 2 was the most potent inhibitor by up to 6-fold over flexible hydrophilic analog 3 and 50-fold over rigid analog 4 (Table I).

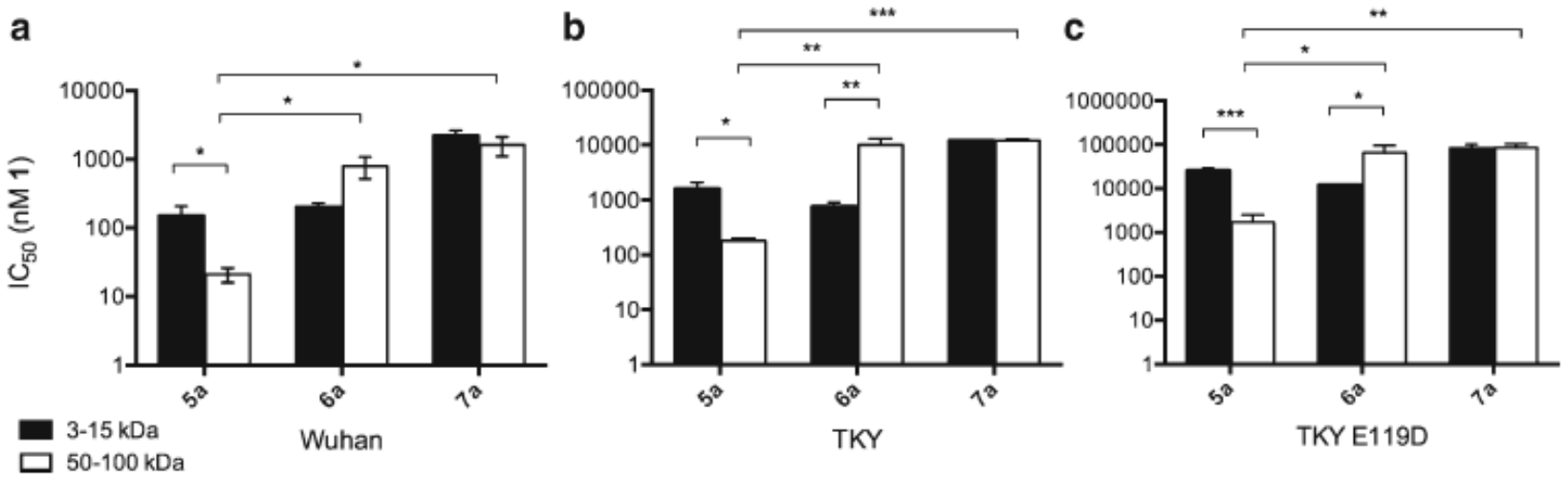


**Fig. 2** $IC_{50}$ values for low-molecular-weight (3–15 kDa; *black bars*) and high-molecular-weight (50–100 kDa; *white bars*) conjugates **5a**-**7a** against (**a**) Wuhan, (**b**) TKY, and (**c**) TKY E119D isolates of influenza A virus. $IC_{50}$ values, reported as nanomolar concentrations of **1**, were determined using the plaque reduction assay after pre-incubation of virus and polymer. Thus, $IC_{50}$ values reflect inhibition of infection. Since $IC_{50}$ values of bare backbones **5**–**7** ranged from 2 to 39 mM, compared to at least 85 $\mu$M for drug conjugates, the polymers themselves had no appreciable antiviral activity. The $IC_{50}$ values for high-molecular-weight **5a** (50–100 kDa) against Wuhan, TKY, and TKY E119D isolates, previously reported by us (11), are included herein for comparison purposes. * $p < 0.05$, ** $p < 0.01$, and *** $p < 0.001$ were determined by a two-tailed Student's *t*-test. All reported values are the mean ± SEM of at least three independent measurements.

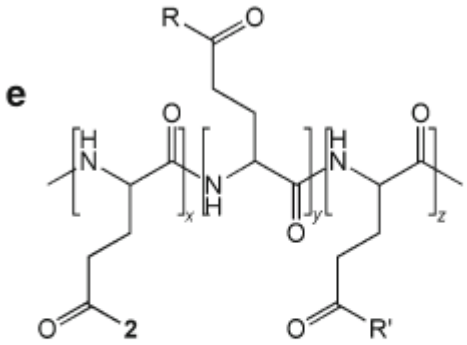


**5a**: $R, R' = NH_2$; $x:(y+z) = 11:89$
**6a**: $R, R' = O^-Na^+$; $x:(y+z) = 11:89$
**7a**: $R = O(CH_2)_2[N(CH_3)_3]^+Cl^-$,
$R' = O^-Na^+$; $x:y:z = 12:45:53$

Conjugate 7a, regardless of molecular weight or viral strain, had the highest IC50 value (Fig. 2). For negatively charged conjugate 6a, the low-molecular-weight inhibitor had an IC50 of up to 4-fold lower than the high-molecularweight conjugate against all three viruses. Conversely, highmolecular- weight 5a was up to 15-fold more potent than the low-molecular-weight variant and up to 75-fold more potent compared to the corresponding charged analogs 6a and 7a.

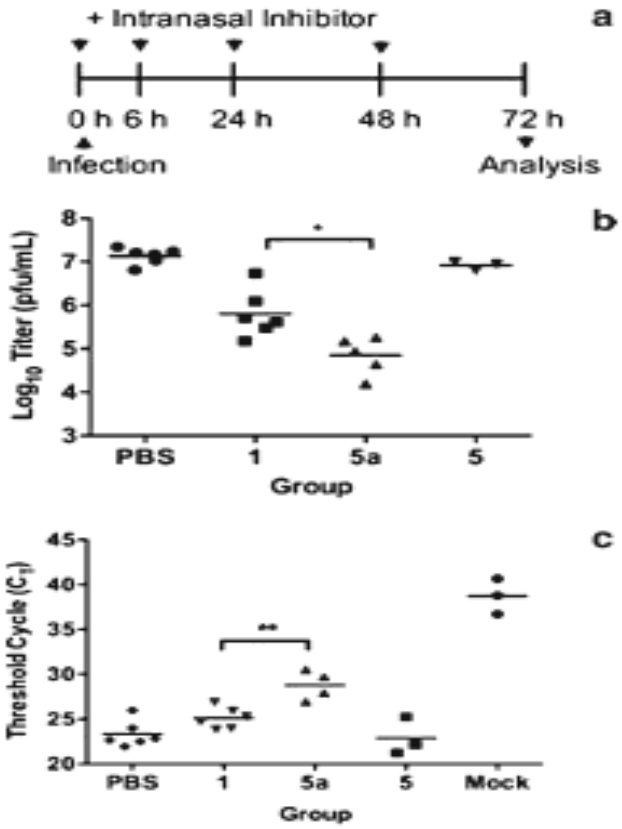


**Fig. 3** (**a**) Experimental design to determine the efficacy of high-molecular-weight **5** and **5a** in mice. (**b**) Viral titers (pfu/mL) from plaque assay of lung homogenates from mice infected with the WSN strain. Equimolar doses of **1** and **5a** were used; a 40-fold higher dose of backbone **5** was included as a control. The PBS group was infected and given vehicle only. Mice were dosed intranasally, immediately infected intranasally, and dosed again at 6, 24, and 48 h p.i.; their lungs were harvested 72 h p.i. Mock-infected group, not shown here due to scale, exhibited no plaques. (**c**) Viral load in lung homogenates of mice infected with PR8 strain. $C_T$ values (higher numbers reflect lower relative levels of viral RNA expression) from qRT-PCR of lung homogenates. The mock group was given only the vehicle. Experimental design was the same as in part (**b**). $^{*}p < 0.05$ and $^{**}p < 0.01$ were determined by two-tailed Student's *t*-test. All reported values are the mean of at least three independent measurements.

We determined viral titers from lung homogenates ofWSNinfected mice using the plaque assay. Untreated mice had high titers of 107 pfu/mL (Fig. 3b). When treated with 1, the titers dropped 20-fold. Upon treatment with a molar equivalency (in terms of 1) of polymeric conjugate 5a, the titers plummeted 190-fold, whereas no decrease was detected from treatment with poly-L-glutamine (5) alone. Thus 5a is some 10-fold more potent than 1 at inhibiting WSN infection in mice.

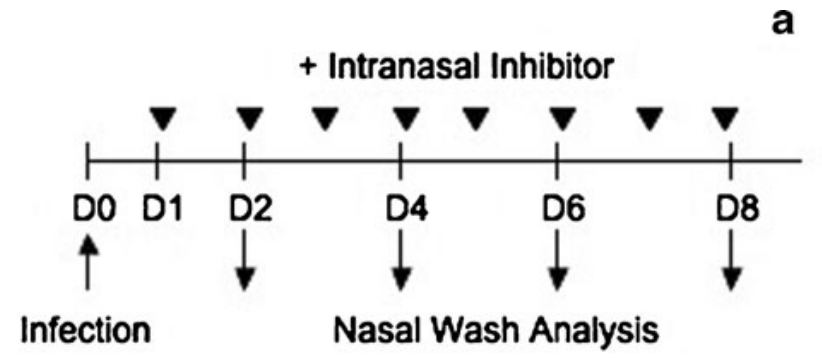


Thus, polymeric conjugate 5a is a more effective therapeutic agent than 1 in this highly relevant ferret model of influenza infection.

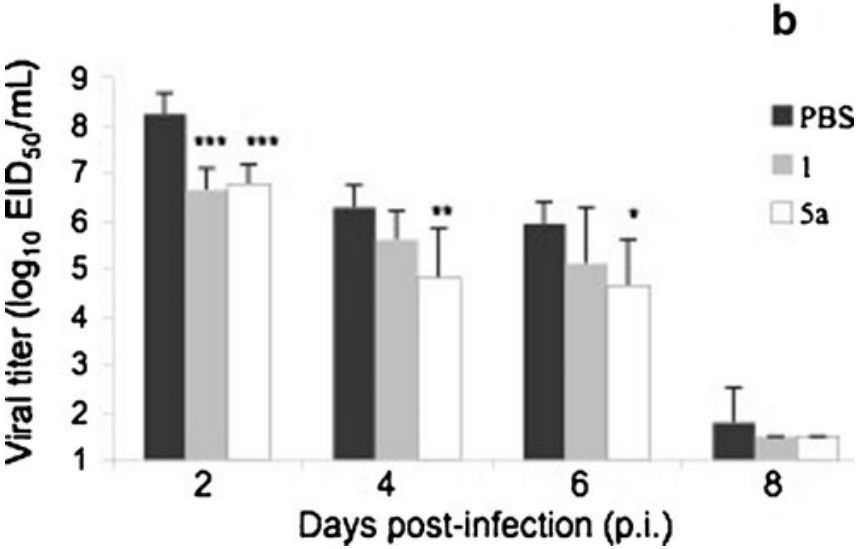


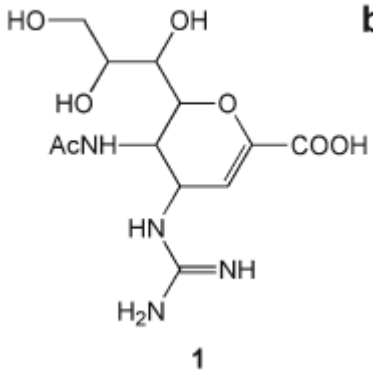


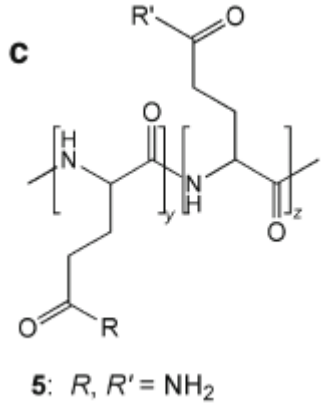


Fig. 4 (a) Experimental design to determine therapeutic efficacy of highmolecular-weight 5a in **ferrets (dağ gelinciği-because this animal model of influenza infection accurately reflects virus infectivity and antiviral activities in humans)** . (b) Viral titers in nasal washings of ferrets infected with Nanchang strain of influenza virus. Groups were treated with vehicle (PBS; black bars; n=6), or equimolar doses of 1 (grey bars, n=6) or 5a (white bars, n=6). Statistically significant differences between PBS control and treated groups are represented by * $p<0.05$ and ** $p<0.01$ as determined by two-tailed Student's t-test. Mean values ± SEM represent triplicate measurements.

**Table II** Drug-Specific Serum Immunoglobulin ELISA Titers From Mice Treated with High-Molecular-Weight High-Dose **5a** or PBS (As a Control) Measured Pre-Challenge ("Pre-"), 10 Days After Primary Challenge ("Primary"), and 10 Days After Secondary Challenge ("Secondary")

| Capture antigen | Time point (relative to challenges) | Reciprocal specific antibody titers[a] | | | | | |
|---|---|---|---|---|---|---|---|
| | | IgG | | IgM | | IgA | |
| | | PBS | **5a** | PBS | **5a** | PBS | **5a** |
| **1** | Pre- | <20 | <20 | <20 | <20 | <20 | <20 |
| | Primary | <20 | <20 | <20 | <20 | <20 | <20 |
| | Secondary | <20 | <20 | 20 | 20 | <20 | <20 |
| **5** | Pre- | <20 | <20 | 20 | 20 | 20 | 20 |
| | Primary | <20 | <20 | 20 | 20 | 20 | 20 |
| | Secondary | <20 | <20 | 20 | 20 | 20 | 20 |
| **5a** | Pre- | <20 | <20 | <20 | <20 | <20 | <20 |
| | Primary | <20 | <20 | 20 | <20 | 20 | <20 |
| | Secondary | <20 | <20 | 20 | 20 | 20 | 20 |
| **5b** | Pre- | <20 | <20 | 40 | 40 | 20 | 20 |
| | Primary | <20 | <20 | 40 | 20 | 20 | 20 |
| | Secondary | <20 | <20 | 40 | 40 | 20 | 20 |

[a] The titers are reported as the reciprocal of the least dilute sample with signal 2-fold above background and are the average of at least two measurements of each sample within each group ($n = 3$). Serum dilutions were 1:20, 1:40, and 1:100

Finally, we examined whether repeated dosing with highmolecular- weight 5a induced immune responses, which could render 5a ineffective. Although small molecules, such as 2, do not typically elicit an antibody response, as part of a polymeric conjugate they can behave as haptens and become immunogenic (26–28). To assess this possibility, we challenged mice intranasally for 4 days with a daily dose of PBS (as a control) or 40 μg of 5a (which was 40 fold higher than what was used to inhibit virus infection in mice). Ten days after the first administration serum samples were collected. To increase the probability of antibody induction, after 4 weeks the mice were rechallenged for 3 days with PBS or 40 μg of 5a daily, and sera were again collected 10 days later. Using 2, 5, and 5a as capture antigens in an ELISA assay, we tested for the presence of specific IgG, IgM, and IgA in the serum samples. Only a background level of immunoglobulin was detected in themice given 5a before, after primary, and after secondary challenge, the same as in control mice given PBS (Table II).

no neutralizing antibodies against 5a or any of its components were observed.